doi:10.1093/plphys/kiab375 PLANT PHYSIOLOGY 2021: 0: 1–26

Plant Physiology®

Research Article

Long-term acclimation to cadmium exposure reveals extensive phenotypic plasticity in Chlamydomonas

Stanislas Thiriet-Rupert,[1,†] Gwenaëlle Gain,[1,2] Alice Jadoul,[1] Amandine Vigneron,[1] Bernard Bosman ,[3] Monique Carnol,[3] Patrick Motte,[1] Pierre Cardol ,[2] Cécile Nouet [1] and Marc Hanikenne [1,*,‡]

1 InBioS-PhytoSystems, Functional Genomics and Plant Molecular Imaging, University of Liège, 4000 Liège, Belgium
2 InBioS-PhytoSystems, Genetics and Physiology of Microalgae, University of Liège, 4000 Liège, Belgium
3 InBioS-PhytoSystems, Laboratory of Plant and Microbial Ecology, University of Liège, 4000 Liège, Belgium

*Author for communication: marc.hanikenne@uliege.be
†Present address: Unité de Génétique des Biofilms, Département Microbiologie, Institut Pasteur, Paris, France.
‡Senior author.

M.H. conceived and directed the research. M.H., S.T., C.N., A.J., G.G., and P.C. designed experiments. A.J., G.G., S.T., C.N., P.C., B.B., and M.C. performed experiments. S.T., G.G., M.H., P.C., A.J., P.M., and A.V. analyzed and interpreted the data. S.T., G.G., and M.H. generated all Figures and Supporting Information material. S.T., M.H., and P.C. wrote the manuscript, with comments of all authors.
The author responsible for distribution of materials integral to the findings presented in this article in accordance with the policy described in the Instructions for Authors (https://academic.oup.com/plphys/pages/general-instructions) is Marc Hanikenne.

Abstract

Increasing industrial and anthropogenic activities are producing and releasing more and more pollutants in the environment. Among them, toxic metals are one of the major threats for human health and natural ecosystems. Because photosynthetic organisms play a critical role in primary productivity and pollution management, investigating their response to metal toxicity is of major interest. Here, the green microalga Chlamydomonas (*Chlamydomonas reinhardtii*) was subjected to short (3 d) or chronic (6 months) exposure to 50 μM cadmium (Cd), and the recovery from chronic exposure was also examined. An extensive phenotypic characterization and transcriptomic analysis showed that the impact of Cd on biomass production of short-term (ST) exposed cells was almost entirely abolished by long-term (LT) acclimation. The underlying mechanisms were initiated at ST and further amplified after LT exposure resulting in a reversible equilibrium allowing biomass production similar to control condition. This included modification of cell wall-related gene expression and biofilm-like structure formation, dynamics of metal ion uptake and homeostasis, photosynthesis efficiency recovery and Cd acclimation through metal homeostasis adjustment. The contribution of the identified coordination of phosphorus and iron homeostasis (partly) mediated by the main phosphorus homeostasis regulator, Phosphate Starvation Response 1, and a basic Helix-Loop-Helix transcription factor (Cre05.g241636) was further investigated. The study reveals the highly dynamic physiological plasticity enabling algal cell growth in an extreme environment.

Introduction

The release of trace metal elements by anthropogenic activities into the environment is one of the most significant threats to human health, as well as water and soil ecosystems (Nagajyoti et al., 2010). Essential metals [iron (Fe), copper (Cu), zinc (Zn), manganese (Mn), etc.] are micronutrients of critical importance for the correct functioning of living cells through their roles as cofactors for many enzymes (Palmer and Guerinot, 2009; Nouet et al., 2011;

Received May 21, 2021. Accepted July 17, 2021. Advance access publication August 16, 2021
© American Society of Plant Biologists 2021. All rights reserved. For permissions, please email: journals.permissions@oup.com

Downloaded from https://academic.oup.com/plphys/advance-article/doi/10.1093/plphys/kiab375/6353050 by guest on 24 August 2021

Thomine and Vert, 2013). However, these essential micronutrients are toxic at supraoptimal concentrations. In contrast, nonessential metals, such as lead (Pb), mercury (Hg), or cadmium (Cd), have toxic effects at low concentrations (Warren, 1989). With the exception of the diatom *Thalassiosira weissflogii* grown under Zn deficiency, where Cd can act as a cofactor of a carbonic anhydrase (Lane and Morel, 2000; Alterio et al., 2015), these nonessential metals have no known physiological function.

Cd is highly toxic, especially upon long-term (LT) exposure to low concentrations (Satarug et al., 2003, 2010), with carcinogenic, embryotoxic, teratogenic, and mutagenic properties (Hartwig, 2010) and has been associated to severe health disorders in human (Pan et al., 2010; Bernard, 2008). Widespread low-level contamination of soil and water is stemming mostly from anthropogenic sources, e.g. mining, nonferrous metal manufacturing, or the application of phosphate fertilizers and sewage sludge on soils. Although Cd emissions into the environment have declined in many industrialized countries, it is still prevalent in emerging countries and low-level contamination of soils still results in important contamination of the food chain (Clemens et al., 2013). Although Cd has multiple harmful effects, affecting the cell from its ultrastructure to its metabolism, the mechanisms underlying Cd toxicity are not clear. Cd exposure seems to induce oxidative stress (Stohs and Bagchi, 1995; Nagajyoti et al., 2010; Yadav, 2010), but since Cd is a nonredox-active metal (Stoiber et al., 2013), reactive oxygen species (ROS) are produced indirectly. Lipid, protein, and nucleic acid damages were also reported under Cd exposure (Watanabe et al., 2003) and, in photosynthetic organisms, growth inhibition and a decrease of chlorophyll (Chl) content were observed (Nagajyoti et al., 2010; Yadav, 2010).

Investigating the response of photosynthetic organisms to metal toxicity is cardinal because of their critical role in primary productivity and pollution management (Pinto et al., 2003; Monteiro et al., 2011; Rawat et al., 2011). In this context, Chlamydomonas (*Chlamydomonas reinhardtii*), as a model unicellular photosynthetic organism, is a highly relevant experimental model (Hanikenne, 2003; Merchant et al., 2007). Cd toxicity in Chlamydomonas is characterized by ultrastructural modifications including starch accumulation, cytoplasmic vacuolization, formation of cytoplasmic electron-dense granules (Nishikawa et al., 2003; Aguilera and Amils, 2005), cell volume increase, development of membranous organelles, or cell-wall volume increase (Visviki and Rachlin, 1994), as well as growth inhibition (Prasad et al., 1998; Hanikenne et al., 2001, 2005b; Jamers and Coen, 2009). Since a fraction of Cd accumulates in the unique chloroplast of Chlamydomonas (Nagel et al., 1996), functions related to this organelle are strongly affected. Indeed, about one-third of the soluble proteins involved in photosynthesis decrease upon Cd exposure, including Rubisco, ferredoxin, ferredoxin-$NADP^+$ reductase, and enzymes involved in the Calvin cycle and Chl biosynthesis (Gillet et al., 2006). Moreover, Cd^{2+} ions were shown to compete for binding to Photosystem II (PSII) calcium (Ca^{2+}) site during the assembly of the water-splitting complex (Faller et al., 2005). These disturbances of plastid-related functions result in impaired photosynthesis (Faller et al., 2005; Vega et al., 2006; Perreault et al., 2011). An impact on proteins involved in carbohydrate and lipid metabolism, amino acid, and protein biosynthesis was also identified (Gillet et al., 2006).

So far, no transporter specific to Cd^{2+} ions has been identified. However, as a divalent cation, Cd^{2+}enters the cell via essential metal transporters (Shahid et al., 2017). For instance, in Arabidopsis (*Arabidopsis thaliana*), Cd can be transported by Iron-Regulated Transporter 1 (IRT1), a ferrous ion transporter of the Zrt-, Irt-like proteins (ZIPs) family, and that an increase of Fe availability induces a decrease of Cd uptake (Rogers et al., 2000; He et al., 2017). In Chlamydomonas, the homolog ZIP transporters IRT1 and IRT2 are induced by Fe deficiency, suggesting an involvement in Fe uptake (Hanikenne et al., 2009; Urzica et al., 2012). Similar to plants, ATP-binding cassette (ABC) transporters were also involved in Cd tolerance in Chlamydomonas (Hanikenne et al., 2001; Faller et al., 2005; Hanikenne et al., 2005b; Wang and Wu, 2006). A higher concentration of Ca, cobalt, or Zn in the culture medium provides protection to Chlamydomonas by decreasing Cd uptake (Mosulén et al., 2003; Lavoie et al., 2012). This competition of Cd for divalent cation transporters perturbs essential metal homeostasis of the cell, which in turn impacts the whole cell functioning.

When exposed to pollutants such as Cd, organisms are able to induce a variety of stress mechanisms allowing acclimation. In Chlamydomonas, the first level of defence is the hydroxyproline and glycoprotein-rich cell-wall, which has high affinity for metal cations (Collard and Matagne, 1990). However, this passive barrier seems to be saturated at environmental Cd concentration (Macfie et al., 1994) and cell-wall-deficient strains accumulate less Cd than the wild-type (WT) (Macfie et al., 1994; Penen et al., 2017). Once inside the cell, different types of mechanisms are used to cope with Cd. Antioxidant defence is enhanced, with the induction of the expression and activity of antioxidant enzymes (Gaur and Rai, 2001; Pinto et al., 2003; Aksmann et al., 2014). Strategies including active efflux, bioconversion into less harmful forms, such as the intracellular chelation by thiolated peptides like phytochelatins, were also widely studied (Howe and Merchant, 1992; Gaur and Rai, 2001; Hanikenne et al., 2005b; Wang and Wu, 2006; Lavoie et al., 2009; Bräutigam et al., 2011). Other effective intracellular chelators used by cells to sequester metal ions are polyphosphates (Rachlin et al., 1984; Seufferheld et al., 2008; de Lima et al., 2013). In the microalgae *Chlamydomonas acidophila* and Chlamydomonas, polyphosphates are thought to bind Cd in the cytoplasm allowing its sequestration into acidic vacuoles (Nishikawa et al., 2003; Blaby-Haas and Merchant, 2014; Penen et al., 2017). More generally, a crosstalk seems to connect metal and phosphorus (P) homeostasis since intracellular concentrations of essential metal under Cd exposure differ depending on P availability in Chlamydomonas (Wang and Dei, 2006; Webster et al., 2011).

Downloaded from https://academic.oup.com/plphys/advance-article/doi/10.1093/plphys/kiab375/6353050 by guest on 24 August 2021

Little data are available on the effect of LT, chronic, exposure to Cd in Chlamydomonas (Yu et al., 2018, 2020). In this study, we used growth assays, ionomic and transcriptomic profiling, photosynthesis analysis, as well as mutant characterization to examine in detail the response to 6-month Cd exposure compared to a 3-d Cd exposure. We examined whether a chronic exposure triggers acclimation mechanisms allowing algae to better face Cd-induced toxicity. We also evaluated the reversibility of these responses. We confirmed that the cell wall and the photosynthetic apparatus are key targets of Cd and showed that coordinated regulation of the P and Fe homeostatic networks is required for proper acclimation to Cd.

Results

Cultures of Chlamydomonas were grown for 6 months in liquid TAgP medium in the absence or presence of 50 μM Cd. TAgP is a modification of the classical Tris–Acetate–Phosphate (TAP) medium (Harris et al., 2009) where inorganic phosphate was replaced by β-glycerophosphate (TAgP) to avoid Cd-P complex formation (Collard and Matagne, 1990). Following this acclimation time, the response of cells to four growth conditions were compared: (1) control condition (Ctrl, six months growth without Cd); (2) control cultures exposed for 3 d to 50 μM Cd (short-term [ST] exposure); (3) 6 months acclimated cultures (LT exposure); and (4) the exact same acclimated cultures subsequently grown for three days in the absence of Cd (Recovery) to investigate the recovery phase upon Cd removal (Supplemental Figure S1). Note that "ST" is used here in opposition to "LT" and already represents an acclimation response in a unicellular organism dividing every 8–12 h. Detailed phenotyping was then conducted to examine the impact of these treatments on algae physiology, including cell growth, total Chls, cell morphology, ionomic profile, and photosynthesis efficiency, supported by a transcriptomic analysis by RNA sequencing (RNA-Seq).

Pre-acclimation decreases the phenotypic impact of Cd exposure

ST exposure (50 μM Cd) during 3 d resulted in 30% lower biomass relative to the Ctrl. In contrast, this reduction was only ∼12% upon LT exposure, similar to the recovery condition (Figure 1A; Supplemental Figure S2).

In agreement with previous reports showing that Cd induced chlorosis (Nagajyoti et al., 2010; Yadav, 2010), a 30% decrease of total Chl content was observed after ST exposure, whereas the LT acclimated cultures had similar Chl levels than the Ctrl cells (Figure 1B). Recovery induced a 15% increase of the Chl content (Figure 1B).

Cd induced the formation of cell aggregates, upon both ST and LT exposures, which persisted upon recovery (Supplemental Figure S3A). In addition, groups of two or four cells surrounded by a common matrix were observed in these three conditions. Such formations were previously observed in Chlamydomonas cultures exposed to stress conditions and are called palmella (Figure 1, C and D; Supplemental Figure S3B; Iwasa and Murakami, 1969; Lurling and Beekman, 2006; Jamers and Coen, 2009; Boyd et al., 2018; Samadani and Dewez, 2018; Cheloni and Slaveykova, 2021; Li et al., 2021). Palmella are originated from dividing cells that remain grouped within the matrix after mitosis (Nakamura et al., 1975). Very few of such structures were observed in the Ctrl, but they appeared in ST cultures, became largely dominant upon LT exposure to Cd and their frequency decreased during recovery (Figure 1, C and D). In addition, loss of motility and increased cell volume were observed in presence of Cd, as described (Visviki and Rachlin, 1994; Hessen et al., 1995; Khona et al., 2016).

Next, the effects of Cd on the ionome of the cells (Salt et al., 2008) were examined. Cellular Cd concentrations [∼0.85 nmol/optical density measurement at 750 nm (OD_{750})] were equivalent in ST- and LT-treated cells and no Cd was detected in cells both in Ctrl and after recovery (Figure 1E). Compared to Ctrl, ST, and LT exposed cells shared a similar ionome profile with higher Cu, Zn, and Mn, but lower Ca and Mg concentrations (Figure 1F). Cd exposure only slightly increased Fe cellular concentration, whereas K concentrations were either lower (ST) or higher (LT) than in Ctrl (Figure 1F). The effects of Cd on the ionome were almost reversed upon recovery, with only K remaining high and Ca readjusting to a higher level.

Some differences in the ionome of ST and LT exposed cells were also observed. Although Fe was only moderately affected, ST-exposed cells contained significantly lower Ca, K, Mg, Zn, and Cu, but higher Mn. This dynamic suggested that the response initiated at ST progressed after LT exposure reflecting either an aggravation of Cd-induced deleterious effects, or an acclimation.

Cd deeply remodels the transcriptome

To examine the molecular mechanisms underlying the phenotypic responses to Cd, three biological replicate samples for each of the four growth conditions were subjected to a transcriptomic analysis using RNA-Seq. A principal component analysis (PCA) of gene expression profiles in each condition showed a clear segregation of the samples (Figure 2A). PC1 and PC2 explained 59% and 30% of the gene expression variance by separating conditions according to (1) the presence or absence of Cd in the culture medium (PC1) or (2) whether or not the cells were pre-acclimated to Cd (PC2), respectively.

Then, differentially expressed genes (DEGs; $\log_2$ fold-change >1 or less than -1; false discovery rate (FDR) adjusted $P < 0.05$) were identified in four specific comparisons (Figure 2B; Supplemental Dataset S1 and Supplemental Figure S4): between ST (1) or LT (2) exposed cells and Ctrl, characterizing the ST and LT responses to Cd exposure, respectively, and between 3 d recovered cells and LT exposed (3) or Ctrl (4) cells, characterizing the recovery response to Cd exposure or the residual response to Cd exposure following recovery, respectively.

Downloaded from https://academic.oup.com/plphys/advance-article/doi/10.1093/plphys/kiab375/6353050 by guest on 24 August 2021

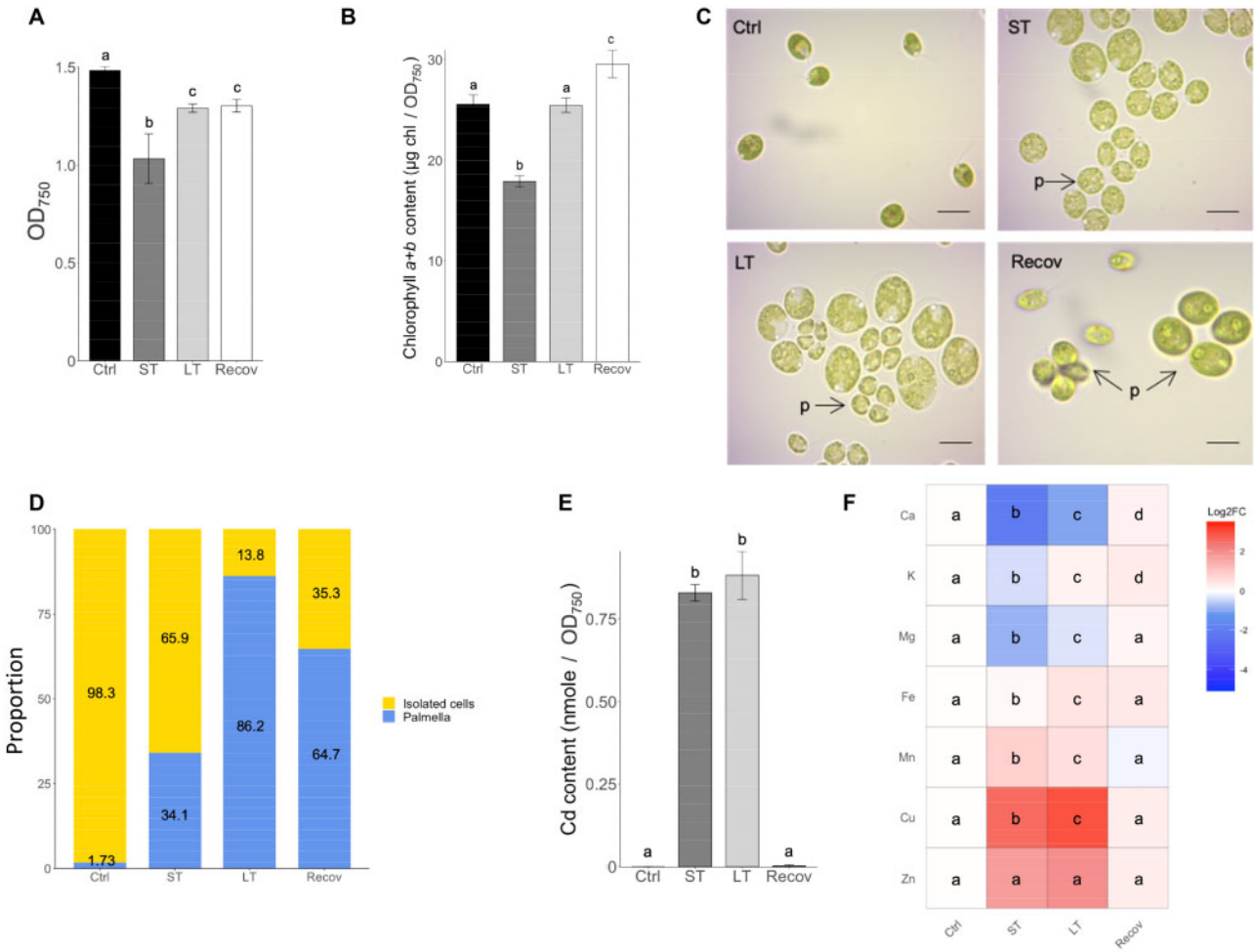

Figure 1 Phenotypic characterization of the control and Cd-exposed cultures. Control cultures grown for 6 months without Cd (Ctrl), ST (3 d) Cd-exposed cultures, LT (6 months) Cd-exposed cultures and recovery cultures (6 months Cd-exposed cells grown for 3 d without Cd) were characterized. A, Biomass estimation and (B) Chl content after 3 d of treatment. Values are means ± SD of three biological replicates. Significant differences ($P < 0.05$) according to one-way ANOVA followed by Tukey's test are shown by different letters. C, Microscopic observations of each culture after 3 d of treatment, palmella (p) are indicated by an arrow. Scale bars = 15 µm. The pictures are representative of three biological replicates. D, Proportion of palmella and isolated cells in each condition after 3 d of treatment. Values are from the observation of 10 fields at the microscope ($n > 900$). E, Cell Cd concentrations after 3 d of treatment. F, Heatmap of the $\log_2$ fold-change of mineral element concentrations in ST, LT, and Recovery cultures relative to the Ctrl. Values are means (± SD in E) of three biological replicates and statistical differences are shown with different letters, according to one-way ANOVA followed by Tukey's test.

Interestingly, shared DEGs were identified among the different responses allowing their classification into seven specific groups of genes (Figure 2C, Gp 1–7). Groups 1 and 2 represented DEGs characterizing the ST and LT responses to Cd exposure, respectively, whereas group 3 contained DEGs common to both ST and LT responses. The latter characterized the core acclimation response to Cd exposure, while group 2, containing nearly half of all identified DEGs, represented genes progressively regulated by Cd. DEGs of group 4 were specific to the recovery response, being regulated by the transition from LT exposure to an absence of Cd. Group 5 genes were common to ST and recovery response, possibly related to the acclimation to ST changes in culture conditions. Group 6 corresponded to genes specifically regulated upon Cd removal, whereas group 7 included genes, which remained differentially regulated compared to Ctrl 3 d after recovery.

To gain further insight into the mechanisms involved in each of the described responses, a Gene Ontology (GO) enrichment analysis was carried out (Supplemental Dataset S2), completed by a detailed manual examination of the DEGs (Table 1). Special attention was paid to functions related to the phenotypic traits shown above to be impacted by the treatments (Figure 1).

Within the 188 DEGs of the ST response, a notable enrichment was found for metal ion transport ($P = 0.0003$), Fe ion transport ($P = 0.01$), superoxide metabolic process ($P = 0.04$), and calmodulin-dependent protein kinase activity ($P = 0.0001$; Supplemental Dataset S2). Moreover, six genes involved in cell-wall synthesis, eight genes involved in chloroplast- and photosynthesis-related processes, six genes responsible for Fe homeostasis and many transporters were highlighted by the manual analysis (Table 1). Nine genes

Downloaded from https://academic.oup.com/plphys/advance-article/doi/10.1093/plphys/kiab375/6353050 by guest on 24 August 2021

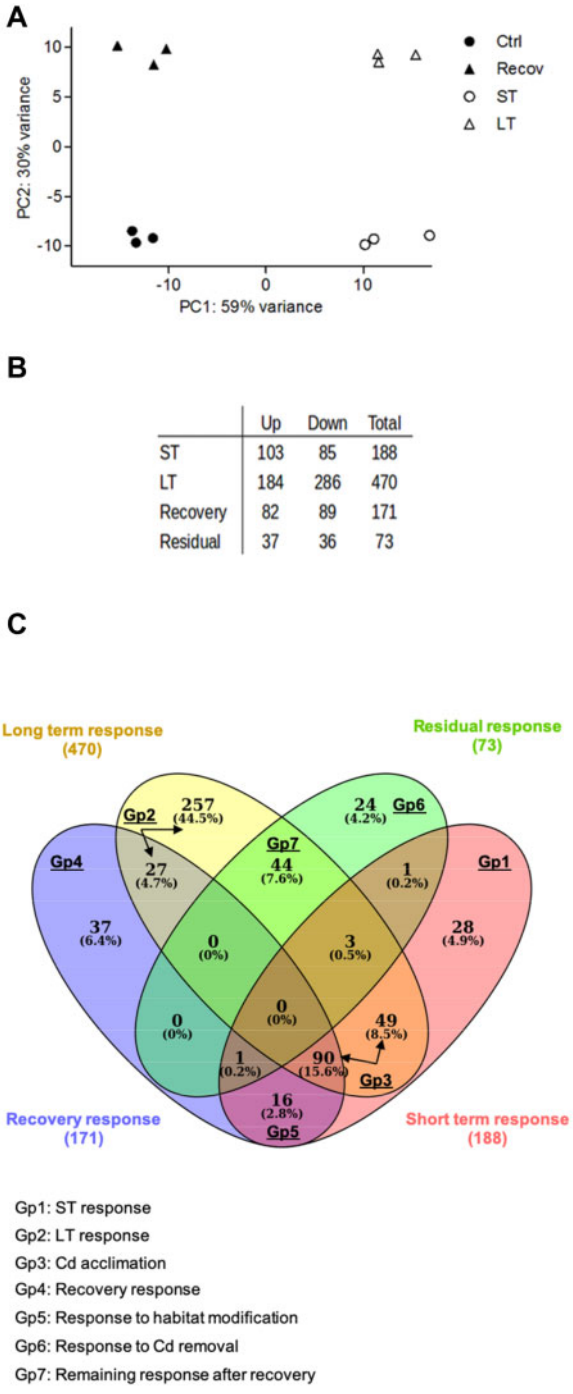

Figure 2 Transcriptomic analysis of the Cd ST, LT, and recovery responses. A, PCA of RNA-Seq gene expression data of control (Ctrl) cultures without Cd, ST (3 d) Cd-exposed cultures, LT (6 months) Cd-exposed cultures, and recovery cultures (6 month Cd-exposed cells grown for 3 days without Cd). B, Number of up-, downregulated, and DEGs ($\log_2$ fold-change >1 or less than −1; FDR adjusted $P < 0.05$) in ST (control versus 3 d Cd-exposed cells), LT (control versus 6 month Cd-exposed cells), Recovery (6 month Cd-exposed cells versus 6 month Cd-exposed cells grown for 3 d without Cd), and Residual (control versus 6 month Cd-exposed cells grown for 3 d without Cd) responses. C, Venn diagram of the identified DEGs for the four responses described in (B), and defining seven sub-groups (Gp) of genes and their potential contribution in those responses. Numbers are numbers of DEGs for each response.

related to P homeostasis were also identified [six transporters, two phosphatases, and one transcription factor (TF)] and signal transduction was well represented with 15 DEGs (Table 1).

The LT response analysis revealed a persistence of metal ion transport ($P = 0.005$), Fe ion transport ($P = 0.03$), and calmodulin-dependent protein kinase activity ($P = 0.0008$) functional categories, as well as the emergence of other categories, including Cu ion transport ($P = 0.003$), Fe homeostasis ($P = 0.03$), porphyrin-containing compound biosynthesis ($P = 0.03$), and cell-wall catabolism ($P = 0.04$; Supplemental Dataset S2). Functions revealed by the manual analysis were shared with the ST response (Table 1). Among the key functions common to ST and LT responses (Gp3, Figure 2C) were cell-wall synthesis, chloroplast, and photosynthesis, Fe homeostasis, ion transport, P homeostasis, and signal transduction (Table 1). The LT response mobilized more genes for these functions, together with a diversification of the functions, illustrating progressive and deepened acclimation to Cd with time, as highlighted by the comparison of Gp1, Gp2, and Gp3 in Table 1.

As more than half of the 171 DEGs of the recovery response were shared with the ST and LT responses, a large overlap of enriched functional categories was observed (Table 1; Supplemental Dataset S2). Interestingly, light harvesting and chloroplastic translation were identified among the 37 Recovery-specific DEGs (Gp4, Figure 2C) by both GO enrichment ($P = 0.0004$ and $P = 0.001$, respectively; Supplemental Dataset S2) and manual analyses (Table 1).

Finally, no GO enrichment was observed in the residual response, with the manual analysis revealing 10 genes related to cell-wall synthesis as regulated in this group.

Overall, the transcriptomic analysis pinpointed functions (e.g. Fe homeostasis, photosynthesis, cell wall) that were directly related to the phenotypes observed in the four growth conditions. It also uncovered additional functions (e.g. P metabolism) not investigated so far in our analysis. These functions were then examined in detail to further understand acclimation to Cd exposure in Chlamydomonas.

Chloroplast and photosynthesis are major targets of Cd toxicity

Several DEGs involved in photosynthesis and other chloroplast-related functions were identified in all four studied responses. Only a few photosynthesis-related genes were impacted, mostly downregulated, upon ST Cd exposure (Figure 3A). Among those, only *FNR1* was directly related to the photosynthetic machinery and displayed significantly diminished expression (Figure 3A). *FNR1* encodes a ferredoxin-$NADP^+$ reductase, which reoxidizes the photosystem I (PSI) direct acceptor, ferredoxin (FDX1). This was concomitant with a decrease in several photosynthesis-related parameters: the amount of Chl (Figure 1B), the relative amount of active photosystems (PSI and PSII) per Chl (Figure 3B), and the relative electron transport rate (rETR) of PSII (Figure 3C).

Downloaded from https://academic.oup.com/plphys/advance-article/doi/10.1093/plphys/kiab375/6353050 by guest on 24 August 2021

Table 1 Manual annotation of the functional categories involved in the Cd ST, LT, and recovery responses

Functional categories	ST response		LT response		Recovery response		Residual response		Gp1		Gp2		Gp3		Gp4		Gp5		Gp6		Gp7	
	Up	Down	Up	Down	Up	Down	Up	Down	Up	Down	Up	Down	Up	Down	Up	Down	Up	Down	Up	Down	Up	Down
Cell wall																						
Synthesis	5	1	6	12	4	6	4	10	2		2	8	2		1	1	1		1	6	1	4
Degradation			2	3				1			2	2										1
Chloroplast and photosynthesis																						
Light harvesting				4	7							4			4							
NPQ			1				1														1	
Electron transfer		2	2		2	1					1		1		1			1				
Rubisco activation				1								1										
Chl synthesis				6	1							6										
Chl degradation	1	1	1	1	1	1							1	1								
Carotenoid synthesis				2	1							2										
Apparatus assembly		1		1	1									1								
Prot transport to chloroplast			1		1						1											
Chaperone	1		1		1								2									
Translation		1		1	6							1			5			1				
Other		1			1													1				
Fe homeostasis	6		8			6			1		1		5									
Transport																						
Ca			1				1														1	
K		2		1						1				1								
N				3	1							3										
P	1	5	1	6	2							1	1	5								
Fe	5		4			4					1		5									
Cu	1		3			2					2		1									
Zn		1	1	1	1						1			1								
Mn	1		1			1							1									
Heavy metals			1								1											
Other	2	3	4	7		1				2	2	6	2	1								
Phosphatase		2		3	2			1						2								1
Transcription	5	3	5	11	3	5		2	1		3	6	3	3		1	1			1		1
Translation		1	1	3			2				1	2		1					2			
Amino acid metabolism	4	2	5	9		2					1	7	4	2								
Metal chelation, phytochelatin	1		1			1							1									
Oxidative stress response	1	1	1	2	2	1						1	1	1	1							
Carbohydrates																						
Anabolism	1			2	3				1			2			2							
Catabolism	1		2	8	3	1		2			1	7	1			1				1		1
Lipids																						
Anabolism	2	1	2	4	3	1						4	1	1	1		1					
Catabolism	1	1		8		1	1					7	1	1		1			1			
Signal transduction	7	8	6	24	2	4	1	2	3		3	15	3	8		2				1		1

The numbers of upregulated and downregulated genes belonging to each functional category in the ST (control versus 3 d Cd-exposed cells), LT (control versus 6 month Cd-exposed cells), Recovery (6 month Cd-exposed cells versus 6 month Cd-exposed cells grown for 3 d without Cd), and Residual (control versus 6 month Cd-exposed cells grown for 3 d without Cd) responses, as well as in each sub-group defined in Figure 2C, are indicated. The sign (up or down) of regulation for genes present in groups overlapping with the Recovery response (Gp2, 3, and 5) is indicated according to the ST and LT responses: the upregulated genes in these two responses are downregulated in Recovery.

Downloaded from https://academic.oup.com/plphys/advance-article/doi/10.1093/plphys/kiab375/6353050 by guest on 24 August 2021

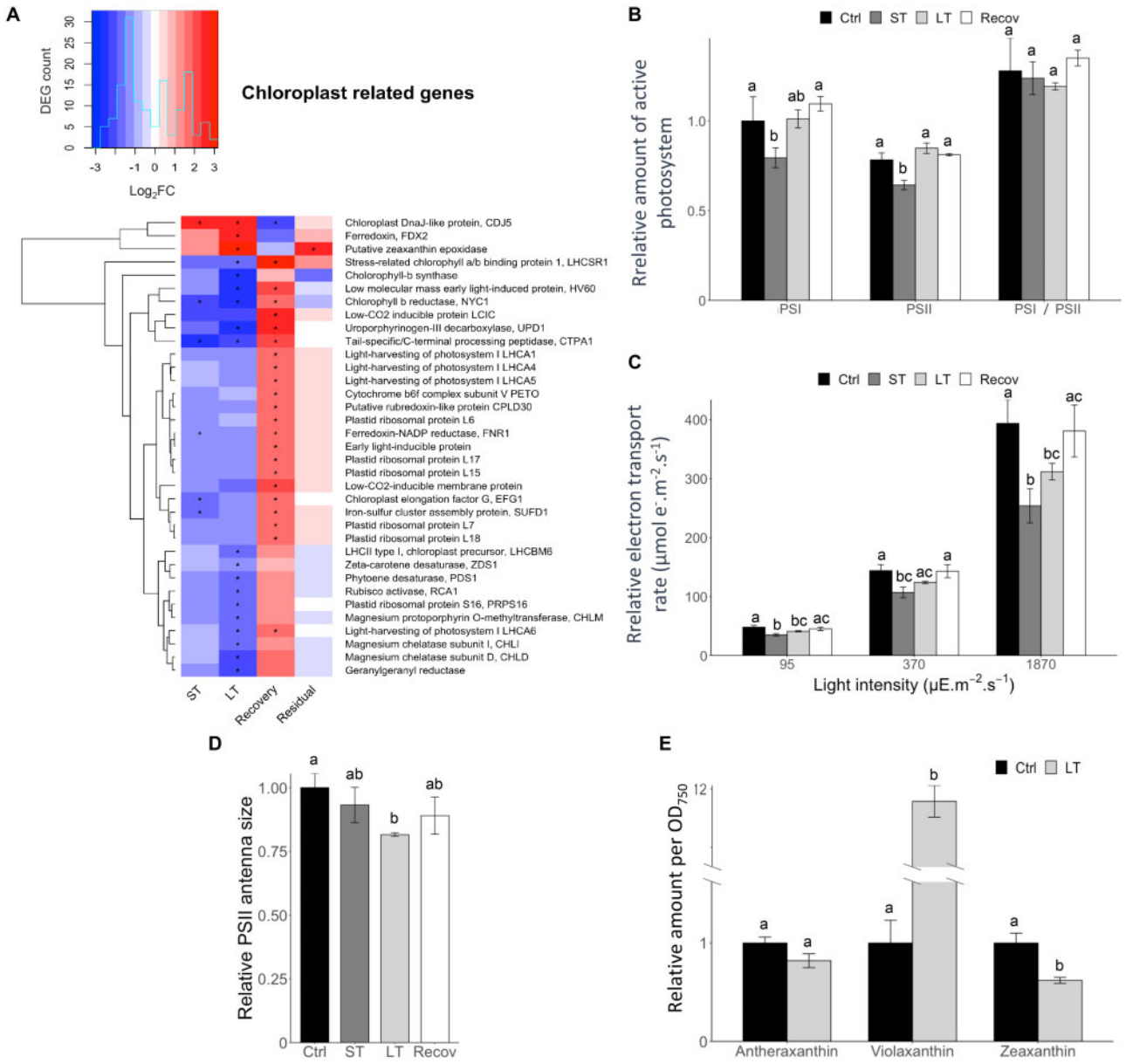

Figure 3 Impact of Cd on the expression of chloroplast-related genes and on photosynthesis. A, Heatmap of chloroplast-related gene expression (Log_2 fold-change) in ST (control versus 3 d Cd-exposed cells), LT (control versus 6 month Cd-exposed cells), Recovery (6 month Cd-exposed cells versus 6 month Cd-exposed cells grown for 3 d without Cd), and Residual (control versus 6 month Cd-exposed cells grown for 3 d without Cd) responses. Significant differences are marked by asterisks (detailed in Supplemental Dataset 1). B, Relative amount of PSI, PSII, and PSI/PSII ratio in control (Ctrl) cultures without Cd, ST (3 d) Cd-exposed cultures, LT (6 months) Cd-exposed cultures and recovery cultures (6 months Cd-exposed cells grown for 3 d without Cd). C, rETR of PSII and (D) relative PSII antenna size in Ctrl, ST, LT, and Recovery cultures exposed to three different PPFD (95, 370, 1,870 µE m^{-2} s^{-1}). E, Relative concentration of xanthophyll cycle pigments in Ctrl and LT cultures after 7 d of Cd treatment. The values are normalized relative to the Ctrl (0 µM Cd). The *Y* axis is log scaled. Values are mean ± SD of three biological replicates. Significant differences ($P < 0.05$) according to one-way ANOVA followed by Tukey's test are shown by different letters.

In contrast, following LT exposure, a larger set of genes was differentially expressed. The expression of five genes coding for enzymes involved in different steps of the Chl or carotenoid biosynthesis pathways (*CHLD*, *CHLI*, *CHLM*, *ZDS*, *PDS*) was significantly decreased, together with three genes encoding light-harvesting complex proteins (*LHCA6*, *LHCSR1*, and *LHCBM6*; Figure 3A; Supplemental Dataset S1). The latter was in agreement with slightly decreased (20%) PSII antenna size upon LT Cd exposure (Figure 3D). However, surprisingly, the amount of photosystems (Figure 3B) and the overall PSII activity (Figure 3C) were restored in this condition, which may explain the better fitness of the cells compared to the ST exposure (Figure 1A).

Moreover, a gene encoding a putative zeaxanthin epoxidase, which plays an important role in the xanthophyll cycle allowing nonphotochemical quenching and protection from

Downloaded from https://academic.oup.com/plphys/advance-article/doi/10.1093/plphys/kiab375/6353050 by guest on 24 August 2021

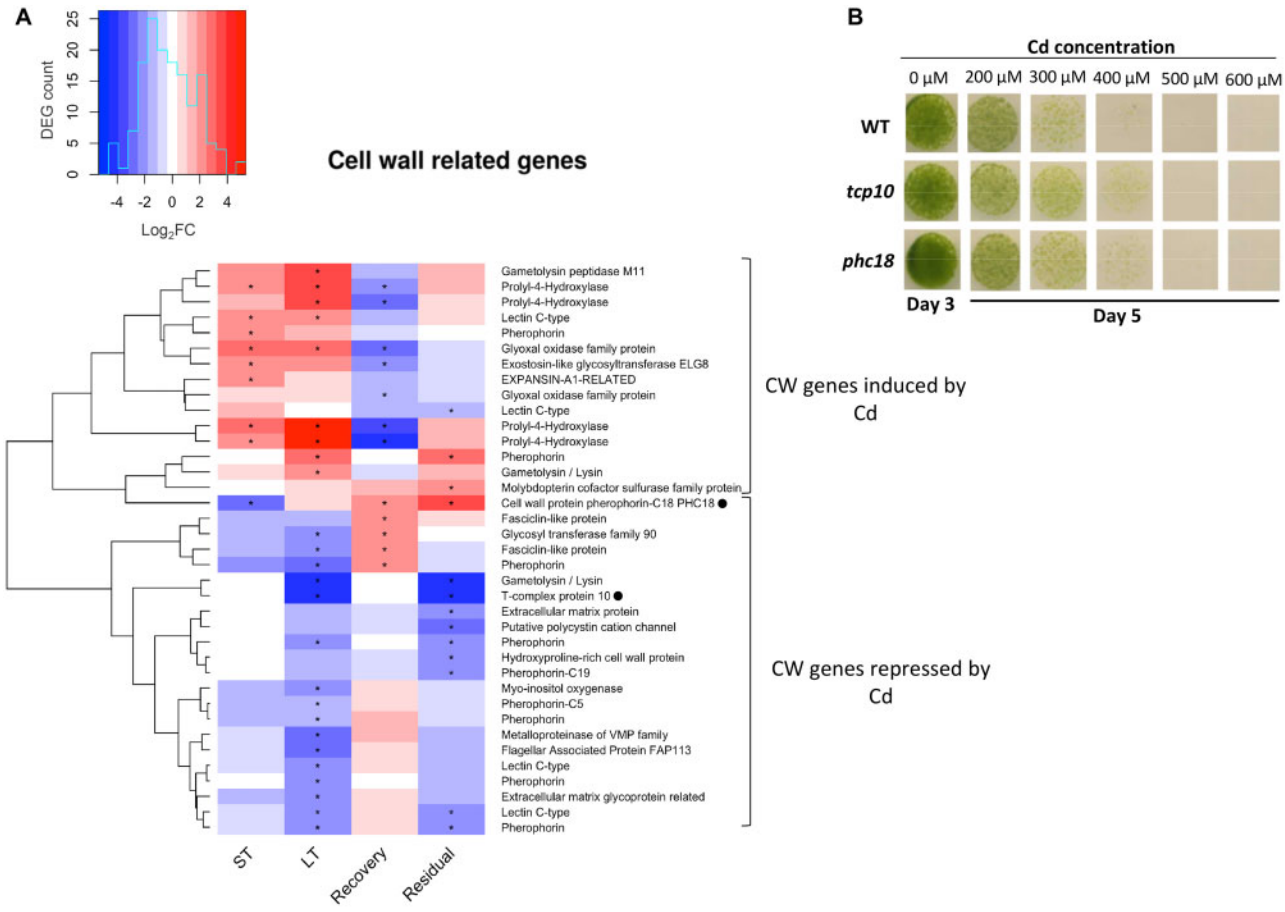

Figure 4 Impact of Cd on the expression of cell-wall-related genes. A, Heatmap of cell-wall-related gene expression (Log_2 fold change) in ST (control versus 3 d Cd-exposed cells), LT (control versus 6 month Cd-exposed cells), Recovery (6 month Cd-exposed cells versus 6 month Cd-exposed cells grown for 3 d without Cd), and Residual (control versus 6 month Cd-exposed cells grown for 3 d without Cd) responses. Significant differences are marked by asterisks (detailed in Supplemental Dataset S1). Two sub-groups of genes that up- or downregulated by Cd are indicated. B, Cd tolerance test on agar plates for *tcp10* and *phc18* mutants. WT, *tcp10*, and *phc18* cells (10^5 cell/ml) were spotted in three replicates on agar plates supplemented with different Cd concentrations (0, 200, 300, 400, 500, and 600 µM, respectively). Pictures were taken after 3 and 5 d of growth and are representative of the three biological replicates.

photooxidative damage (Havaux and Niyogi, 1999; Baroli et al., 2003; Havaux et al., 2007), was upregulated in LT conditions. This enzyme ensures the production of violaxanthin from zeaxanthin through antheraxanthin. While zeaxanthin content was slightly lower in LT exposed cells than in Ctrl cells, violaxanthin content was 10 times higher (Figure 3E). This suggested that an increased pool of xanthophyll pigments plays a significant role in Cd acclimation in LT conditions.

After the recovery phase, an almost complete reversal of the Cd-induced responses at ST and LT was observed, with genes downregulated in the presence of Cd being upregulated in the recovery response (i.e. returning to a control state) and vice versa (Figure 3A). Accordingly, neither PSII antenna size (Figure 3D), the amount of PS (Figure 3B) nor the overall PSII activity (Figure 3C) was different from the Ctrl.

The cell wall is important for Cd tolerance

Many genes involved in cell wall synthesis and degradation were differentially regulated in all four experimental conditions (Figure 4A), with a more or less equal number of up- and downregulated genes (Table 1). More precisely, a set of genes was upregulated after ST Cd exposure, and this response was maintained at LT, whereas another set of genes was downregulated after LT exposure (Figure 4A). This suggested that cell-wall remodeling plays a role in Cd tolerance in Chlamydomonas as previously shown in other plant species (Krzesłowska, 2011).

A large majority of these genes were differentially expressed in the LT and Residual responses (groups 2, 6, and 7 in Figure 2C), accounting for 79% of cell wall-related DEGs (Table 1). This suggested an important role of the cell wall in LT tolerance to Cd. Moreover, many of these genes induced in presence of Cd were repressed after the recovery phase, and reciprocally (Figure 4A).

To further investigate the role of the cell wall in Cd tolerance in Chlamydomonas, mutants for two candidate genes were obtained from the Chlamydomonas Stock Center (Li et al., 2016b): (1) *TCP10* (T-Complex Protein 10, Cre06.g303200), which was downregulated in LT and Residual responses and (2) *PHC18* (pherophorin C-18,

Downloaded from https://academic.oup.com/plphys/advance-article/doi/10.1093/plphys/kiab375/6353050 by guest on 24 August 2021

Cre24.g755997), which was downregulated in ST response and upregulated in Recovery and Residual responses. These genes were selected based on their distinct regulation profile and their putative role as constituents of the cell wall. In particular, PHC18, a pherophorin belonging to a glycoprotein family specific to the *Chlamydomonadales*, is an essential component of the complex extracellular matrix (ECM) in *Volvox carteri*, which is modulated in response to environmental changes (Hallmann, 2006). TCP10 has not been characterized in detail, but was shown to be differentially regulated in a cell cycle mutant (Tulin and Cross, 2015).

Exposure to 50 μM Cd for 3 d in liquid cultures had no impact on the growth, Chl content and ionome profile of the mutants compared to Ctrl conditions and to the WT. However, both mutants displayed a slight but reproducible increased tolerance to 300 and 400 μM Cd on agar plates, compared to the WT (Figure 4B; Supplemental Figure S5), consistent with the downregulation of their gene expression by Cd (Figure 4A). This suggests that both cell-wall genes play a role in Cd acclimation in Chlamydomonas.

P homeostasis-related genes are downregulated upon Cd exposure

Several P homeostasis-related genes were differentially regulated in ST, LT, and Recovery conditions (Supplemental Dataset 1; Figure 5A). Following ST exposure, the gene encoding the P deficiency master regulator Phosphate Starvation Response 1 (PSR1; Wykoff et al., 1999; Rubio et al., 2001; Moseley et al., 2006) was downregulated, as well as those encoding the intracellular PHO1 phosphatase, four Na^+/Pi symporters (including PTB2/8/12 animal-like high-affinity Pi transporters), and a periplasmic phosphate binding component of a phosphate ABC transporter, while the plant-like high affinity H^+/Pi cotransporter PTA3 was upregulated. This gene regulation profile was maintained after LT exposure, with in addition the downregulation of the genes encoding the PTB4 Na^+/Pi symporter and PHOX, an extracellular alkaline phosphatase, and was mostly reversed upon recovery. This strong downregulation of P uptake-related genes would supposedly result in a decrease of P cellular content in response to Cd exposure. Surprisingly, the total P content was only significantly lower in ST-exposed cells compared to Ctrl cells, whereas it was significantly higher after the recovery phase (Figure 5B). However, these genes were identified based on their homology with the yeast Pi uptake system (Moseley et al., 2006) and since no cellular localization or functional characterization was carried out for *PTA* or *PTB* genes in Chlamydomonas, the interpretation of their regulation is difficult.

It is interesting to note that the Chlamydomonas PSR1 TF is homologous to the Arabidopsis PHR1 (Phosphate Starvation

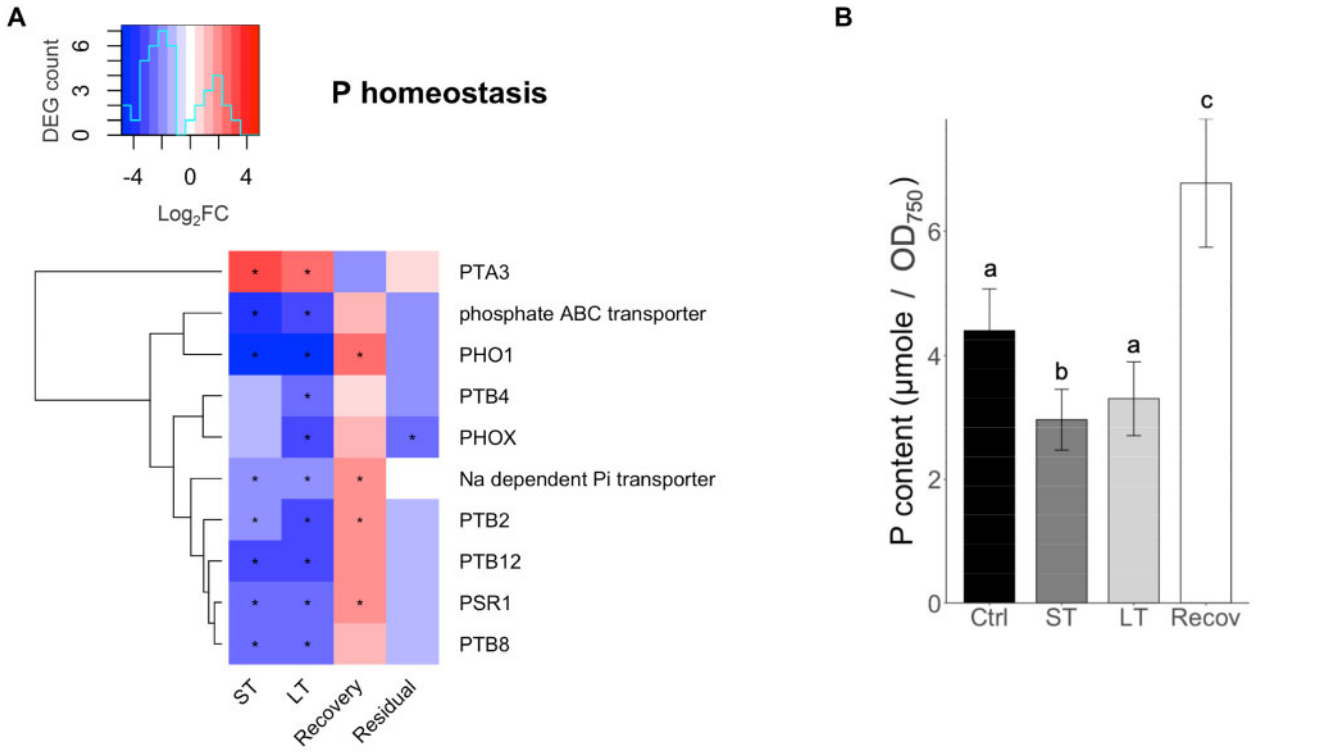

Figure 5 Impact of Cd on phosphorus homeostasis. A, Heatmap of P homeostasis-related gene expression (Log_2 fold change) in ST (control versus 3 d Cd-exposed cells), LT (control versus 6 month Cd-exposed cells), Recovery (6 month Cd-exposed cells versus 6 month Cd-exposed cells grown for 3 d without Cd), and Residual (control versus 6 month Cd-exposed cells grown for 3 d without Cd) responses. Significant differences are marked by asterisks (detailed in Supplemental Dataset S1). B, P content in control (Ctrl) cultures without Cd, ST (3 d) Cd-exposed cultures, LT (6 months) Cd-exposed cultures, and recovery cultures (6 month Cd-exposed cells grown for 3 d without Cd) Values are mean ± SD of three biological replicates. Significant differences ($P < 0.05$) according to one-way ANOVA followed by Tukey's test are shown by different letters.

Downloaded from https://academic.oup.com/plphys/advance-article/doi/10.1093/plphys/kiab375/6353050 by guest on 24 August 2021

Response 1) TF (Rubio et al., 2001) and that both TFs share well-conserved mechanisms to mediate P homeostasis. As PHR1 is suspected to play a role in metal homeostasis in Arabidopsis (Khan et al., 2014; Briat et al., 2015), this function may also be conserved for the Chlamydomonas PSR1. Since no modification in cellular P content was observed upon Cd exposure, the downregulation of PSR1 could be related to an involvement of this TF in metal homeostasis.

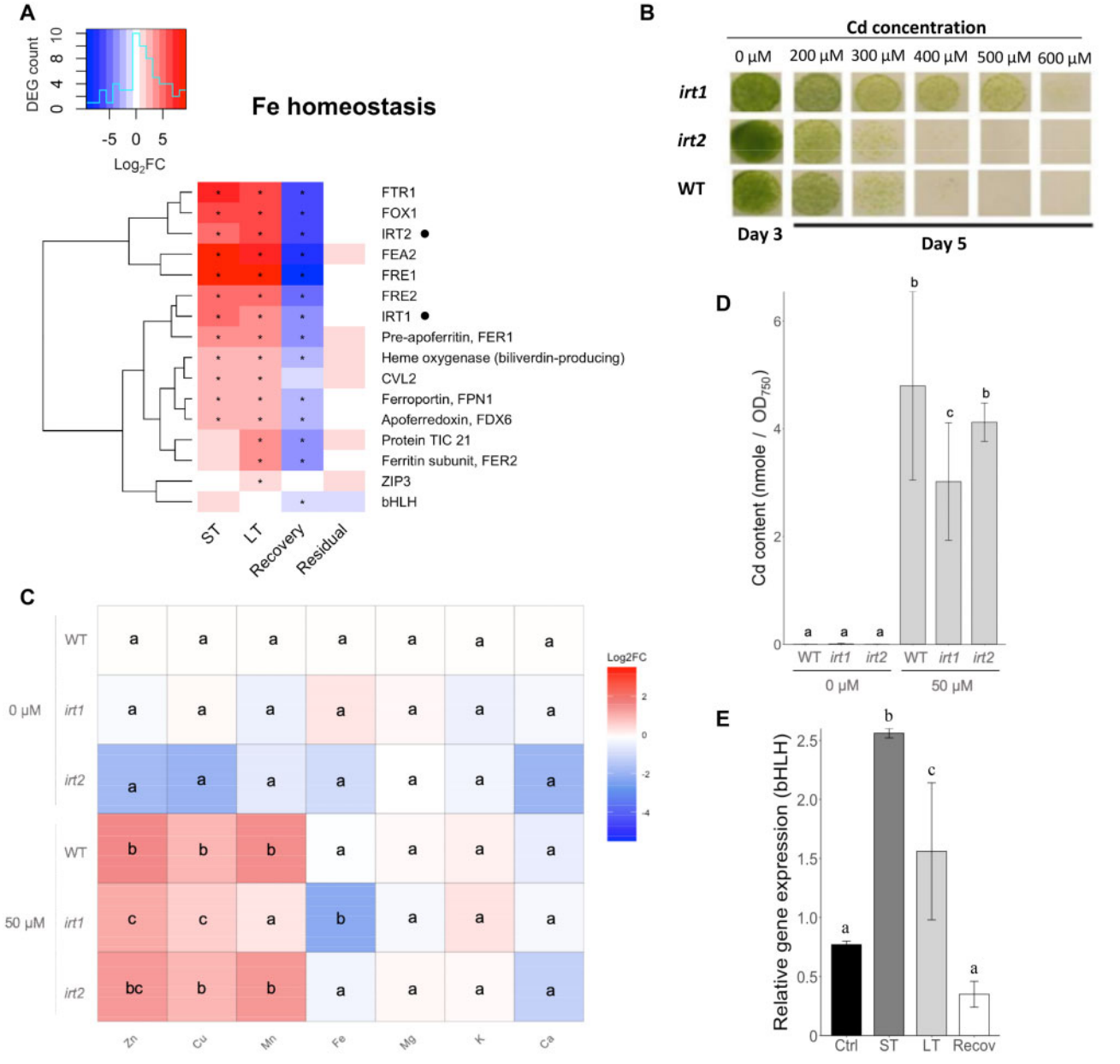

Figure 6 Impact of Cd on iron homeostasis. A, Heatmap of Fe homeostasis-related gene expression (Log_2 fold change) in ST (control versus 3 d Cd-exposed cells), LT (control versus 6 month Cd-exposed cells), Recovery (6 months exposed cells versus 6 month Cd-exposed cells grown for 3 d without Cd), and Residual (control versus 6 month Cd-exposed cells grown for 3 d without Cd) responses. Significant differences are marked by asterisks (detailed in Supplemental Dataset S1). B, Cd tolerance test on agar plates for *irt1* and *irt2* mutants. WT, *irt1*, and *irt2* cells (10^5 cell/mL) were spotted in three replicates on agar plates supplemented with different Cd concentrations (0 µM, 200 µM, 300 µM, 400 µM, 500 µM, and 600 µM, respectively). Pictures were taken after 3 and 5 d of growth and are representative of the three biological replicates. C, Heatmap of the log_2 fold change of mineral element concentrations in the *irt1* and *irt2* mutants in Ctrl (0 µM Cd) as well as in WT and the *irt1* and *irt2* mutants in ST (3 d 50 µM Cd exposure) conditions relative to the WT in Ctrl (0 µM Cd). Statistical differences are shown by different letters ($P < 0.05$) according to one-way ANOVA followed by Tukey's test. D, Cd content of WT, *irt1* and *irt2* mutants in Ctrl (0 µM Cd) and ST (3 d 50 µM Cd exposure) conditions. E, Relative expression level of the Cre05.g241636 gene encoding a bHLH TF in control (Ctrl) cultures without Cd, ST (3 d) Cd-exposed cultures, LT (6 months) Cd-exposed cultures and recovery cultures (6 month Cd-exposed cells grown for 3 d without Cd). D and E, Values are mean ± SD ($n = 3$ biological replicates). Significant differences ($P < 0.05$) according to one-way ANOVA followed by Tukey's test are shown by different letters.

Downloaded from https://academic.oup.com/plphys/advance-article/doi/10.1093/plphys/kiab375/6353050 by guest on 24 August 2021

Fe deficiency-responsive genes are upregulated upon Cd exposure

After ST Cd exposure, a large set of genes involved in Fe homeostasis was upregulated. This included genes involved in both low-affinity Fe^{2+} (*IRT1* and *IRT2*; Hanikenne et al., 2009; Urzica et al., 2012) and high-affinity Fe^{3+} uptake systems (*FRE1*, *FOX1*, *FTR1*, and *FEA2*; Herbik et al., 2002; La Fontaine et al., 2002; Merchant et al., 2006; Allen et al., 2007a; Hanikenne et al., 2009; Narayanan et al., 2011; Glaesener et al., 2013), which are known to be induced upon Fe deficiency, as well as genes involved in intracellular Fe trafficking and storage (*FRE2*, *FER1*, *CVL2*, and *FPN1*; Singh et al., 2007; Jeong et al., 2008; Urzica et al., 2012; Figure 6A). The same set of genes was upregulated after LT exposure, with in addition the genes encoding the second plastid localized ferritin subunit (FER2) and the putative Zn/Fe transporter ZIP3 (Figure 6A), and all were downregulated upon recovery as for the chloroplast- and cell wall-related genes described above.

As IRT1 and IRT2 are putative Fe^{2+} transporters, possibly also able to transport Cd (as Cd^{2+}) into the cell, Cd tolerance was examined in *irt1* and *irt2* mutants upon Cd exposure (200–600 μM) for 5 d on agar plates. The *irt2* mutant displayed a tolerance level similar to the WT, whereas the *irt1* mutant displayed strongly increased Cd tolerance (Figure 6B). Ionome profiling further revealed that no significant differences were observed between the WT and the *irt1* and *irt2* mutants in control conditions (Figure 6C). In contrast, upon 3 d of growth in liquid culture in the presence of 50 μM Cd, the *irt1* mutant accumulated lower amounts of Cd (Figure 6D), possibly accounting for its increased Cd tolerance. The accumulation of Cu, Zn, and Mn increased in all three genotypes upon Cd exposure, but did significantly less so in the *irt1* mutant (Figure 6C). Fe accumulation was also reduced in the *irt1* mutant in Cd condition.

Finally, a basic Helix-Loop-Helix (bHLH) TF (Cre05.g241636), previously shown to be induced in Fe deficiency condition (Urzica et al., 2012), was identified as moderately regulated by Cd in the RNA-Seq data (Figure 6A). Interestingly, this bHLH TF is related to the Arabidopsis group IVc of bHLH, which is involved in Fe homeostasis regulation (Zhang et al., 2015; Li et al., 2016a; Liang et al., 2017; Naranjo-Arcos et al., 2017). The Cre05.g241636 expression profile was further examined by RT-qPCR, which revealed a strong upregulation of the gene upon ST and, to a lower extent, upon LT, Cd exposure, and its downregulation to control levels upon recovery (Figure 6E).

The PSR1 and Cre05.g241636 bHLH TFs are part of a regulatory network

A potential involvement of the PSR1 and Cre05.g241636 bHLH TFs in metal homeostasis and in the response to Cd exposure was further examined. Motifs corresponding to the Transcription Factor Binding Sites (TFBSs) of their Arabidopsis. homologs were retrieved from PlantTFDB (Jin et al., 2017) and used to search the regulatory sequences (1,000-bp upstream the transcription start site) of the recovery response DEGs. This RNA-Seq dataset was selected as both TFs were found to be differentially expressed in these conditions (Supplemental Dataset S1). Out of the 171 DEGs, 89 and 63 genes were putative targets of Cre05.g241636 or PSR1, respectively, and, among them, 33 were putative targets of both TFs forming a putative co-regulation network (Supplemental Dataset S3; Figure 7).

This in silico analysis identified eight Fe homeostasis genes as putative targets of (1) Cre05.g241636 only (*FTR1* and *FRE1*), (2) PSR1 only (*FRE2* and *FER1*), and (3), interestingly, both TFs (*FER2*, *FOX1*, *FEA2*, and *IRT1*). Similarly, three out of four P homeostasis-related recovery DEGs were also putative targets of both TFs (*PHO1*, *PTB2*, and a Na^+/Pi symporter encoding genes), whereas the fourth gene (encoding a protein phosphatase 2C, PP2C) was only targeted by Cre05.g241636. Five genes related to metal homeostasis (other than Fe) were linked to one of the two TFs: *CTR1* (Cu transporter) and *PCS* (phytochelatin synthase, PCS) were putative targets of PSR1, whereas *CTR2* (Cu transporter), *ZTR1* (Zn transporter), and *NRAMP1* (Fe/Mn transporter) were among the putative targets of Cre05.g241636. Interestingly, the *FSD1* gene encoding the chloroplastic FeSOD isoform, whose activity is reduced under Fe deficiency (Allen et al., 2007b), was also putatively targeted by Cre05.g241636.

Finally, 21 genes with chloroplast-related functions were also identified as targets of PSR1 and/or Cre05.g241636. These genes have diverse functions, including protein transport into the chloroplast, electron transfer, but mainly light harvesting and chloroplastic translation (Supplemental Dataset S3; Figure 7). These genes were mainly specific to the Recovery response (Gp 4 in Figure 2C).

These data indicate that PSR1 and Cre05.g241636 are possibly part of a putative regulatory network, with both TFs controlling overlapping sets of P and metal homeostasis targets. The data also suggest that Cd exposure alters the functioning of the network in Chlamydomonas.

As P and Fe are of critical importance for the development and functioning of photosynthetic cells, we next examined whether such a network has been conserved during the evolution to land plants using publically available transcriptomic data from Arabidopsis (Bustos et al., 2010; Mai et al., 2016). First, we collected expression data for (1) the *phr1phl1* Arabidopsis double mutant exposed to P starvation; PHR1 and PHL1 (PHR1-like) are two key regulators of the P starvation response in Arabidopsis and are homologous of the Chlamydomonas PSR1 TF (Rubio et al., 2001; Bustos et al., 2010) and (2) the *fit* Arabidopsis mutant exposed to Fe sufficiency and deficiency; FIT (FER-like Iron-deficiency-induced TF) is, among multiple bHLH TFs involved in Fe homeostasis in Arabidopsis, a major regulator of the Fe deficiency response (Colangelo and Guerinot, 2004; Brumbarova et al., 2015; Mai et al., 2016). Among all 5,588 mis-regulated genes in the Arabidopsis mutants compared to the WT (Supplemental Dataset S4A), 779 were common to both mutants (Supplemental Dataset S4B). Second, we focused our analysis on root expression data, as it was the

Downloaded from https://academic.oup.com/plphys/advance-article/doi/10.1093/plphys/kiab375/6353050 by guest on 24 August 2021

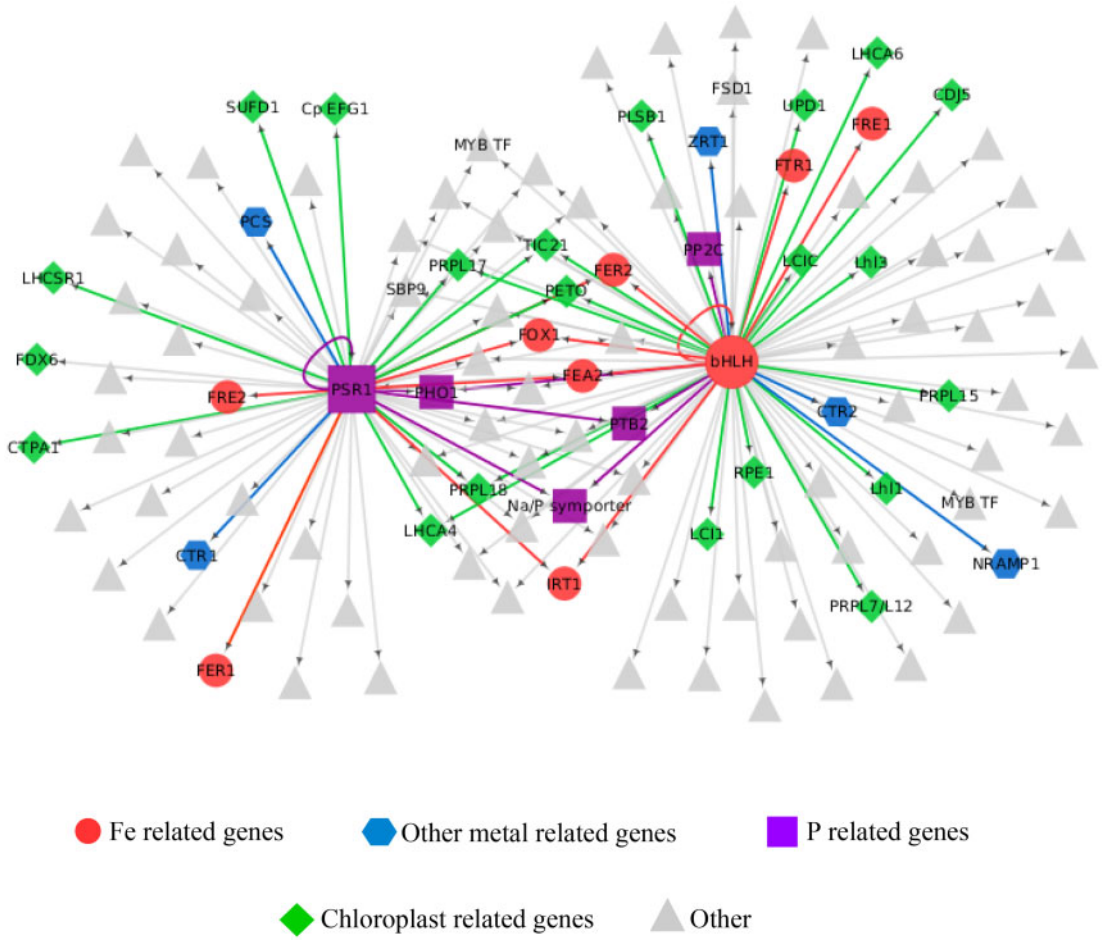

Figure 7 A PSR1 and Cre05.g241636 bHLH transcriptional network. The regulatory network of the PSR1 and Cre05.g241636 bHLH TFs is based on an analysis of TF binding sites in the promoters of genes differentially expressed during the Recovery response (see Figure 2C and "Materials and Methods"). Each node corresponds to a gene and putative regulatory interactions between the TFs and the target genes are symbolized by arrows. Nodes have a specific color and shape based on the functional category of the corresponding genes. Nodes of interest are labeled by the corresponding gene names.

only organ common to both studies and identified 279 overlapping genes (Supplemental Dataset S4C). Interestingly, genes specific to both P and Fe starvation responses in Arabidopsis were included among those 279 overlapping genes suggesting that PHR1, PHL1, and FIT are possibly involved in both responses. Third, to examine this hypothesis in more details, nine Arabidopsis genes were initially selected for promoter analysis (highlighted in yellow in Supplemental Dataset S4C): *IRT1*, *MTP3*, *AHA7*, *VTL5*, and *UGT74E2* are part of the Fe deficiency response in Arabidopsis; *PHT1;4*, *MGD2*, and *PS2* are linked to P homeostasis in Arabidopsis; and FLA15, whose putative ortholog was found in the PSR1 regulon in Chlamydomonas (Supplemental Dataset S3). For four of those Arabidopsis nine genes (*VTL5*, *MGD2*, *PHT1;4*, and *FLA15*), a Chlamydomonas putative ortholog was differentially expressed in the Cd dataset (Supplemental Dataset S1). The promoter sequences (−1,500/+100 bases) of those nine Arabidopsis genes were searched as above for occurrences of the P1BS motif, specific of the P deprivation response, and the E-box motif, specific of bHLH TFs. All nine promoters contained at least one occurrence of both motifs (Supplemental Figure S6; Supplemental Dataset S4, D and E). The data for FIT and the Fe-deficiency genes *IRT1*, *MTP3*, and *AHA7* are in agreement with previously published data (Colangelo and Guerinot, 2004). Fourth, to generalize this observation, we collected promoter sequences of all genes (2,407) mis-regulated in roots of the *phr1phl1* or *fit* mutants exposed to P or Fe deficiency, respectively (Supplemental Dataset S4A), sorted them in three groups, *phr1phl1*-specific (940 genes), *fit*-specific (1,188 genes), or overlapping (279 genes) promoters, and probed those groups of promoters for P1BS or E-box enrichment. An enrichment of P1BS motif in the promoters of the overlapping genes was found relative to *fit*-specific promoters (exact Fisher's test, $P = 0.01$), whereas no difference was observed relative to the *phr1phl1*-specific promoters, suggesting that a P/Fe regulatory network does exists in Arabidopsis. As positive control, the P1BS was also enriched in the *phr1phl1*-specific promoters relative to the *fit*-specific promoters (exact Fisher's test, $P = 2.83e\text{-}5$). The reciprocal analysis was less conclusive.

Downloaded from https://academic.oup.com/plphys/advance-article/doi/10.1093/plphys/kiab375/6353050 by guest on 24 August 2021

No enrichment was observed for the E-box in the overlapping group of promoters of the two specific groups. It may stem from the fact that the E-box motif is short and is the core binding site of all bHLH TFs, i.e. of more than 120 bHLH TFs in Arabidopsis involved in very different functions (Heim et al., 2003; Toledo-Ortiz et al., 2003) including P starvation response (Chen et al., 2007), as opposed to the P1BS motif which is longer and specific to the P response. However, because the genes investigated here (*fit*-specific and *fit*/*phr1phl1* overlap) are mis-regulated in a *fit* mutant, it is very likely that they are under the control of Fe starvation response-related bHLH TFs.

Altogether, this analysis suggests that the regulatory network mediated by PSR1 and a bHLH TF to coordinate P and Fe homeostasis in Chlamydomonas is conserved and possibly even more complex in Arabidopsis.

PSR1 and Cre05.g241636 have a role in Fe homeostasis and chloroplast function regulation

Based on these in silico predictions (Figure 7), mutant lines for the *PSR1* and Cre05.g241636 bHLH genes were obtained from the Chlamydomonas Library Project (CLiP) collection. The two mutants were crossed back with a WT strain and the progenies displayed a ∼1:1 segregation of par^R and par^S, confirming single insertion of the mutagenic cassette in the genome (Supplemental Table S1A). Furthermore, the reduced growth of the *psr1* mutant on a medium with reduced P level co-segregated with the presence of the Par^R cassette in the genome and thus the *psr1* mutation (Supplemental Table S1B). This also further confirmed that despite residual expression of *PSR1* in the *psr1* background (Figure 8A), the mutant displays typical defects in P homeostasis (Wykoff et al., 1999; Moseley et al., 2006).

The two mutants were further phenotyped in detail. First, reverse transcription-quantitative polymerase chain reaction (RT-qPCR) analysis confirmed that, in control conditions, the expression of the *PSR1* and *bHLH Cre05.g241636* genes was strongly reduced in the *psr1* and *bhlh* mutant lines, respectively (Figure 8A), indicating that those two mutants are knockdown strains. Although the two TFs were interconnected in a putative regulatory network, the *bHLH Cre05.g241636* gene expression was not significantly different in the *psr1* mutant, and reciprocally (Figure 8A). Moreover, expression analysis of a selection of putative targets (Figure 7) confirmed that the two TFs are involved in the transcriptional regulation of these genes, at least in control conditions. Indeed, the expression of *FRE1* and *FSD1*, putative targets of the bHLH Cre05.g241636, was significantly upregulated in the *bhlh* mutant whereas the expression of *CTR1*, putative target of PSR1, was downregulated in the *psr1* mutant (Figure 8A). As predicted, the expression of *IRT1*, *FEA2*, and *PHO1* was altered in both mutants. Bulked segregant analysis of pools of 20 Par^R and 20 Par^S progenies from a *psr1* × WT backcross showed that the *PSR1*, *PHO1*, *IRT1*, and *FEA2* genes displayed lower expression levels in the Par^R strains compared to Par^S strains, indicating that their de-regulation co-segregated with the *psr1* mutation (Supplemental Figure S7). Finally, the analysis also revealed that the strong induction of Fe deficiency genes, *FRE1*, *IRT1*, and *FEA2*, upon ST Cd exposure was similar in WT and both *psr1* and *bhlh* mutants, suggesting that additional regulators are involved in the response to Cd.

Second, ionome profiling revealed lower P concentration, as well as higher Cu and Fe concentrations, in the *psr1* mutant in control conditions compared to the WT (Figure 8B), whereas no major alteration was observed in the *bhlh* mutant (Figure 8B). Upon ST Cd exposure, both mutants displayed reduced Cd accumulation compared to the WT, with a significantly lower accumulation in *bhlh* compared to *psr1* (Figure 8C). The Cd treatment resulted in reduced (P, Ca, K, Fe) or increased (Cu, Zn, Mn) accumulation in the WT and the two mutants. However, the amplitude of these changes were different among genotypes: (1) the P and Ca reductions were more pronounced in the *psr1* and *bhlh* mutants, which both displayed an additional reduction of Mg concentration and (2) the increased accumulation of Cu (*bhlh*), Zn (*psr1*, *bhlh*), and Mn (*psr1*, *bhlh*) was of a lower scale in the mutants compared to the WT. The data overall suggested a Cd-induced systemic alteration of the ionome in both mutant backgrounds.

Third, although the *bhlh* and *psr1* mutants had no major growth phenotypes upon Cd exposure (Figure 8D), the *bhlh* mutant displayed distinct Cd sensitivity of the rETR of PSII (Figure 8E; Supplemental Table S2): the *bhlh* mutant maintained a higher rETR than the WT. This phenotype co-segregated with the paromomycin resistance in the progeny of a *bhlh* × WT backcross, indicating that it is linked to the *bhlh* mutation (Supplemental Table S1C). These observations are consistent with the presence of several photosynthesis-related genes among the putative targets of this bHLH TF.

Discussion

Although important progress has been achieved in the last decade in our understanding of the molecular mechanisms underlying Cd uptake and accumulation (Clemens and Ma, 2016; Clemens, 2019), knowledge about the effect of LT, chronic, Cd exposure on photosynthetic organisms remains limited (Yu et al., 2018, 2020). Here, we assessed the response to short (3 d) and long (6 months) Cd exposure in Chlamydomonas, as well as the reversibility of this response. We showed that LT acclimation to Cd relied on molecular pathways similar to the response to short Cd exposure, but mobilized three times more DEGs (Figure 2 and Table 1; Supplemental Figure S4). The CW, adjustment of metal homeostasis (Fe in particular) and photosynthesis, as well as a regulatory network involving the main P homeostasis regulator PSR1 (Rubio et al., 2001) and a bHLH TF (Urzica et al., 2012; Hidayati et al., 2019) contributed to Cd acclimation. These profound physiological alterations enabled restored growth (Figure 1, A and B) and photosynthetic function (Figure 3, B and C). Nevertheless, this response was almost fully reversed within 3 d upon growth in Cd-free medium

Downloaded from https://academic.oup.com/plphys/advance-article/doi/10.1093/plphys/kiab375/6353050 by guest on 24 August 2021

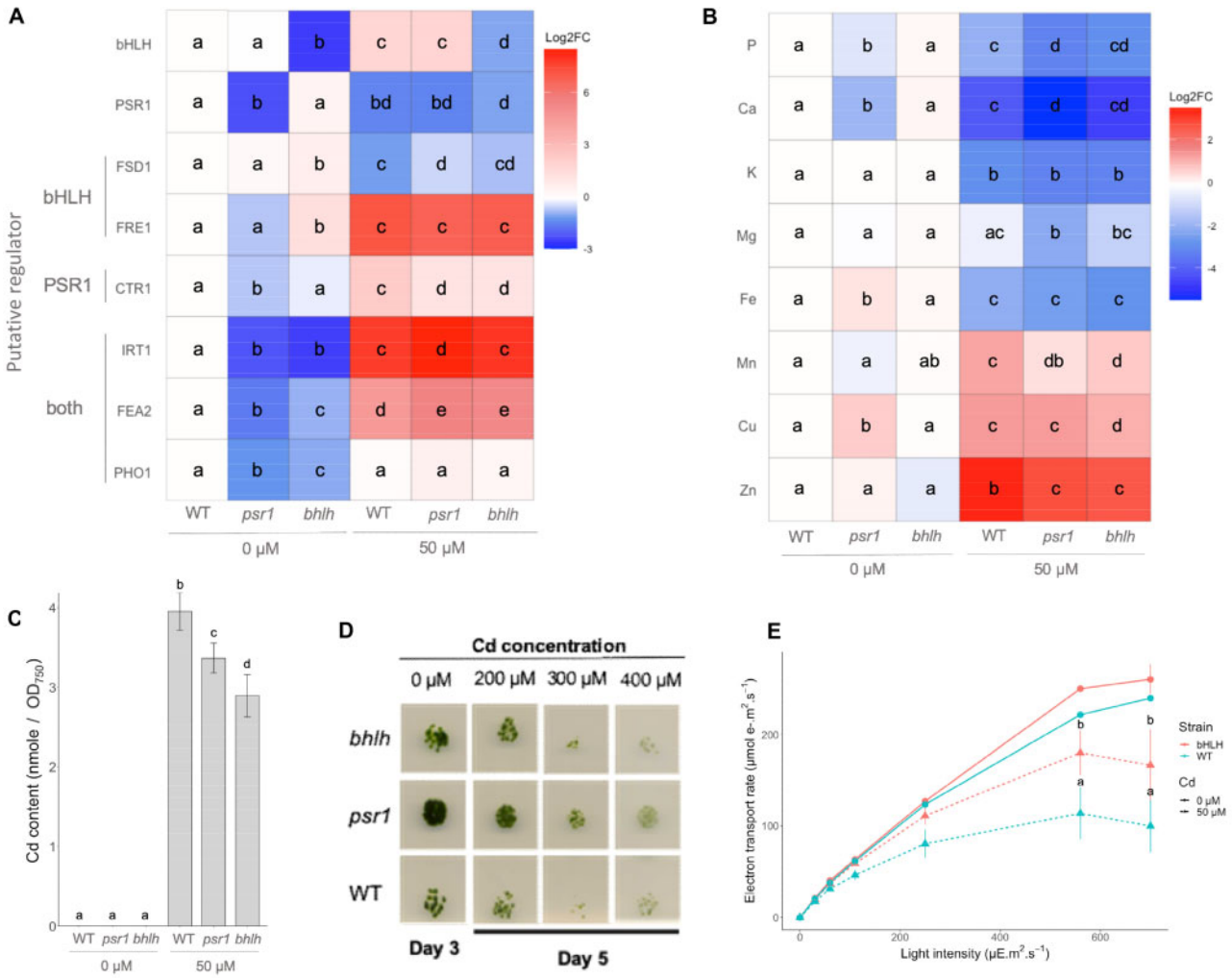

Figure 8 Impact of Cd on *psr1* and Cre05.g241636 *bhlh* mutants. A, B, Heatmaps of the $\log_2$ Fold Change of the relative expression levels of a selection of PSR1 and/or Cre05.g241636 bHLH TF putative target genes (A) and of mineral element concentrations (B) in WT as well as in the *psr1* and *bhlh* mutants in Ctrl (0 µM Cd) and ST (3 d 50 µM Cd exposure) conditions. All $\log_2$ fold changes are relative to the WT in Ctrl (0 µM Cd). Statistical differences are shown by different letters ($P < 0.05$) according to one-way ANOVA followed by Tukey's test. C, Cd content of WT, *psr1*, and *bhlh* mutants in Ctrl (0 µM Cd) and ST (3 d 50 µM Cd-exposure) conditions. Values are mean ± SD (n = three biological replicates). Significant differences ($P < 0.05$) according to one-way ANOVA followed by Tukey's test are shown by different letters. D, Cd tolerance test on agar plates for *psr1* and *bhlh* mutants. WT, *psr1*, and *bhlh* cells (10^4 cell/mL) were spotted in three replicates on agar plates supplemented with different Cd concentrations (0 µM, 200 µM, 300 µM, and 400 µM, respectively). Pictures were taken after 3 and 5 d of growth and are representative of the three biological replicates. E, rETR of PSII in WT and *bhlh* strains exposed to a range of light intensities ($30 - 700$ µE m^{-2} s^{-1}) upon growth in control conditions (0 µM Cd) or in the presence of 50 µM Cd for 3 d. Values are mean ± SD of three biological replicates. Significant differences ($P < 0.05$) according to one-way ANOVA followed by Tukey's test were observed at all light intensities (Supplemental Table S2) but are shown here by different letters for the two highest light intensities only due to lack of space.

(Figure 2; Supplemental Figure S4), concomitantly to a sharp decrease of Cd concentration (Figure 1E), highlighting a major plasticity of metabolic processes in Chlamydomonas. Although new mutations likely appeared in the cultures during the LT Cd exposure, rapid and almost fully reversible response to Cd suggests that acclimation, rather than adaptation, processes are still controlling the cell physiology. Finally, the residual response was mainly dominated by genes involved in CW synthesis and to a lesser extent in signal transduction, translation, and transcription, suggesting that CW remodelling is still perturbed after the recovery phase. This is in line with the observation of palmelloid structures in the corresponding cultures.

Cell-wall remodeling and multicellularity-like structures as a first protection

The Chlamydomonas CW contains pectins and glycoproteins, which have strong binding affinity for metal ions through their carboxylate groups (Haynes, 1980; Collard and Matagne, 1990; Crist et al., 1994), and constitutes a physical barrier providing an efficient protection against toxic metal ions such as Cd (Cain and Allen, 1980; Macfie et al., 1994;

Downloaded from https://academic.oup.com/plphys/advance-article/doi/10.1093/plphys/kiab375/6353050 by guest on 24 August 2021

Penen et al., 2017). Consistently, most CW-related DEGs of the ST Cd response were upregulated and involved in CW maturation and synthesis (Figure 4A and Table 1), possibly increasing the CW buffering capacity. This interpretation has however to be mitigated as a CW-less Chlamydomonas strain was shown to internalize less Cd than the WT (Macfie and Welbourn, 2000), suggesting that the CW binding capacity could facilitate Cd accumulation, possibly by making metal ions available to nonspecific divalent cation transporters located at the cell surface (see below).

So far, the role of the CW following Cd chronic exposure has been under-documented. After LT Cd exposure, the ST response, with mostly upregulated genes, was maintained but was complemented by a strong downregulation of another set of CW-related genes, including several pherophorin-encoding genes (Figure 4A and Table 1). This observation is consistent with the formation of palmelloids upon Cd exposure (Figure 1, C and D; Supplemental Figure S3B). Palmelloids are groups of growing and dividing daughter cells within a unique CW (Nakamura et al., 1975). Palmelloid formation is a typical stress response in Chlamydomonas (Iwasa and Murakami, 1969; Lurling and Beekman, 2006; Jamers and Coen, 2009; Boyd et al., 2018) and was recently reported for Cd exposure (Samadani and Dewez, 2018; Cheloni and Slaveykova, 2021). Cd is indeed known to disturb the cell cycle (Cao et al., 2018). Unlike other responses to LT Cd exposure, palmelloids were maintained upon recovery (Figure 1, C and D), consistently with the presence of many lowly expressed pherophorin genes in the residual response (de Carpentier et al., 2019; Figure 4A, bottom). This suggests that reversion of the palmelloid formation is a slow process or that recovery from a LT acclimation to Cd is a stressful event itself.

In addition to palmelloids, larger aggregates of up to several tens of cells surrounded by a matrix (as defined by de Carpentier et al., 2019) were also observed. Such biofilm-like structures could enable Cd tolerance by preventing Cd access to the cell wall and therefore entering into the cell, as suggested in bacteria (Wu et al., 2015). Noticeably, the Chlamydomonas close relative *Volvox carteri* forms small spherical multicellular colonies (Olson and Nedelcu, 2016) surrounded by a complex ECM, which is modulated in response to environmental changes (Hallmann, 2003; Domozych and Domozych, 2014). Pherophorins are essential components of this ECM (Hallmann, 2006). Interestingly, a gene encoding a volvocine algal *regA* like (VARL) TF (*VARL12*) was among downregulated genes in ST and LT Cd conditions (Supplemental Dataset S1). The VARL protein family is related to RegA (Duncan et al., 2007), a repressor of germ cell fate in *V. carteri* (Kirk et al., 1999), and was only identified in *Chlamydomonadales* and the liverwort *Marchantia polymorpha* (Sharma et al., 2013). Although no function was identified for VARL TFs in Chlamydomonas, the downregulation of *VARL12* in conditions where biofilm-like structures and palmelloids were identified is an interesting feature to further investigate, as it might represent premises towards a form of multicellular organization, which could protect the cells. In this context, cells included in palmelloid structures maintained higher photosynthetic efficiency compared to isolated cells, when exposed to Cd (Supplemental Figure S8).

The key contribution of CW remodeling to Cd acclimation was further confirmed in this study by the analysis of the *phc18* and *tcp10* mutant lines, which both displayed slightly increased Cd tolerance, in agreement with the downregulation of the corresponding genes upon Cd exposure (Figure 4, A and B; Supplemental Figure S5). Further studies will be required to determine how these genes contribute to CW reorganization, palmelloid formation, and control of Cd and nutrient uptake.

Finally, in addition to CW alterations, Chlamydomonas cells displayed other structural changes upon Cd exposure, including motility loss, which is a common reaction under various stressful conditions (Hessen et al., 1995; Khona et al., 2016) and increased cell volume (Figure 1C). The latter was also reported upon chronic Cd exposure in *C. bullosa* (Visviki and Rachlin, 1994), and may result from Cd-induced abnormal cell division.

The uptake and trafficking machinery as a mean to balance Cd-induced metal homeostasis perturbations

As a divalent cation, Cd enters and is distributed within the plant cells via divalent metal transporters with pervasive specificity (for instance, see Vert et al., 2002; Cailliatte et al., 2009; Wong and Cobbett, 2009; Clemens, 2019). Transporters from the same protein families are found in the Chlamydomonas genome (Hanikenne et al., 2005a, 2009; Merchant et al., 2006; Blaby-Haas and Merchant, 2012), and likely also contribute to Cd transport. Therefore, Cd can compete for uptake with other metal nutrients and alters their cellular homeostasis. Consistently, the ionome of Chlamydomonas was strongly impacted upon both ST and LT Cd exposure (Figure 1F), with Cd-induced decreased Ca, K, and Mg, and increased Cu, Zn, and Mn concentrations, respectively (Figure 1F).

Reflecting the need to adjust the homeostasis of those elements, several genes encoding metal transporters were upregulated upon ST and/or LT Cd exposure, including *CTR1* and *CTR2* for Cu (Page et al., 2009), *ZIP3* for Zn and/or Fe (Merchant et al., 2006; Hanikenne et al., 2009) and *NRAMP1* for Mn (Allen et al., 2007b) for instance (Supplemental Dataset S1). Cu, Zn, and Mn levels were down to Ctrl levels after three days of recovery, which is consistent with the downregulation of almost all transporters (Supplemental Dataset S1). Moreover, the Cd-induced reduction of Ca in cells is in line with a previous study (Mosulén et al., 2003) showing that Cd uptake in Chlamydomonas is diminished in the presence of additional Ca in the medium, suggesting competition for the same transporters, as suggested in several species (Clemens et al., 1998; Baliardini et al., 2015; Ahmadi et al., 2018). The same study also highlighted a

Downloaded from https://academic.oup.com/plphys/advance-article/doi/10.1093/plphys/kiab375/6353050 by guest on 24 August 2021

decrease of N uptake upon Cd exposure, which is in agreement with the downregulation of one nitrate and two ammonium transporters following LT Cd exposure (Supplemental Dataset S1).

Those ionome alterations may represent direct responses to Cd (e.g. a modified uptake to out-compete Cd) or may be an indirect effect of the induction of broad specificity transporters. For instance, Cd is known to alter Fe uptake (Lombi et al., 2002; Lešková et al., 2017; Hanikenne et al., 2021). Fe is a key element in respiratory and photosynthetic electron transport as well as for Chl synthesis (Nouet et al., 2011). In Arabidopsis, increased Fe in the medium allowed a decrease of Cd uptake (He et al., 2017), and the main Fe^{2+} uptake transporter in roots, the ZIP protein IRT1, was shown to represent a major source of entry for Cd and other divalent cations upon Fe deficiency (Rogers et al., 2000; Vert et al., 2002). In Chlamydomonas, both ST and LT Cd exposure had a major impact on Fe homeostasis, with the induction of 10 and 12 Fe-responsive genes, respectively (Figure 6A). This response involved both Fe^{3+} (*FRE1*, *FOX1*, *FTR1*; Page et al., 2009) and Fe^{2+} (*IRT1*, *IRT2*) uptake systems as well as an accessory gene (*FEA2*; Hanikenne et al., 2009; Narayanan et al., 2011; Glaesener et al., 2013), and genes encoding proteins (possibly) involved in intracellular Fe trafficking and storage (*FER1*, *FER2*, *CVL2*, *ZIP3*, and *FPN1*; Singh et al., 2007; Jeong et al., 2008; Urzica et al., 2012).

Moreover, the *MSD3* gene, encoding a Mn superoxide dismutase, was upregulated following ST and LT exposure and this gene was shown to be induced upon Fe deficiency in Chlamydomonas to compensate the loss of FeSOD activity in the chloroplast (Allen et al., 2007b). Although no Fe deficiency was observed in our experiment, the *MSD3* upregulation may contribute to Fe saving (Page et al., 2012) and is in line with the induction of all other Fe deficiency-related genes. The observed increase in Mn uptake in the presence of Cd (Figure 1F) might provide additional Mn for superoxide dismutases.

This Cd-dependent expression dynamics enabled maintenance of Fe levels in cells after both ST and LT exposure, in contrast to most other nutrient cations (Figure 1F). This response was very rapidly and fully reverted upon Cd removal from LT cultures (Figure 6A). Chlamydomonas thus evolved very dynamic regulatory mechanisms to maintain Fe homeostasis, further illustrating the critical importance of Fe for the cell functioning in the alga.

Among Cd-induced Fe uptake transporters, IRT1 and IRT2 were good candidates for a direct contribution to Cd uptake by the Chlamydomonas cells. Although they belong to another ZIP subfamily (Hanikenne et al., 2005a; Blaby-Haas and Merchant, 2012), IRT1 and IRT2 may indeed play a similar role as their IRT1 counterpart in plants (Vert et al., 2001). While an *irt2* Chlamydomonas mutant had no clear Cd tolerance or ionome phenotypes upon Cd exposure, an *irt1* mutant displayed reduced Cd accumulation upon Cd exposure (Figure 6D), as well as increased Cd tolerance (Figure 6B). The *irt1* mutant also accumulated less Zn, Cu, and Mn upon Cd exposure, suggesting a broad specificity of IRT1. Our data thus strongly suggest that Cd enters the cells via IRT1, which is induced by a Cd-triggered Fe deficiency. Paradoxically, this upregulation may contribute to increased Cd uptake. Proper Fe supply is however maintained thanks to the induction of the Fe^{3+} uptake system that possibly compensates the Fe uptake imbalance.

Finally, our study also highlights *TIC21* as another gene induced by Cd exposure and possibly involved in Fe distribution into the cell (Figure 6A). The homologous gene to *TIC21* in Arabidopsis, *PIC1* (for permease in chloroplasts 1), was suggested to mediate plastid Fe-uptake (Duy et al., 2007, 2011). Although this function remains controversial (Shi and Theg, 2013) and was not demonstrated in algae, *TIC21* displayed an expression profile similar to Fe homeostasis-related genes as it was upregulated upon Cd exposure and rapidly downregulated following the recovery phase (Figure 6A). Interestingly, chloroplastic Fe accumulation triggers the recovery of Cd induced photosynthesis inhibition in plants (Solti et al., 2016). Here, the induction of *TIC21* in LT-exposed cells was concomitant with the restoration of photosynthesis efficiency (Figure 3, B and C). Further work will be needed to determine if TIC21 is involved in the adjustment of Fe supply or protein import into the chloroplast in response to Cd, but its genic expression profile supports an involvement in the Fe deficiency response.

Altogether, as no difference of Cd concentration was observed between ST and LT Cd-exposed cells, the reported adjustments of metal ion uptake seem more important to maintain metal homeostasis than to decrease Cd uptake. Consequently, the improved fitness of LT exposed cells (Figure 1A) may rather be related to a decrease of the harmful effects of Cd.

Photosynthetic adjustments to cope with LT Cd exposure

Once in Chlamydomonas cells, Cd is mainly accumulated in vacuoles and in the chloroplast (Nagel et al., 1996; Penen et al., 2017, 2020). Metal cofactors are critical for the photosynthetic electron transport chain (Nouet et al., 2011) and the Cd-induced metal homeostasis disturbance in the chloroplast directly impacts photosynthesis. This is illustrated by the fact that the photosynthetic capacity was negatively impacted upon ST exposure to Cd (Figure 3, B and C), which presumably accounts for the marked decrease in biomass (Figure 1A). However, the negative impact on the cell photosynthetic capacity does not seem to result from a massive downregulation of the related genes to acclimate to ST Cd exposure (Figure 3A), but more likely results from a physiological impact of Cd. Overall, this ST impact of Cd is in good agreement with the known effects of Cd on photosynthesis (Faller et al., 2005; Gillet et al., 2006; Perreault et al., 2011; Parmar et al., 2013). One of these effects is the degradation of PSI active sites, as illustrated in ST exposed cells (Figure 3B). In this respect, the upregulation of the plastid localized ferritin subunit *FER1* could play a role in buffering

Downloaded from https://academic.oup.com/plphys/advance-article/doi/10.1093/plphys/kiab375/6353050 by guest on 24 August 2021

Fe released by this PSI degradation, as it was suggested for Fe deficiency (Busch et al., 2008; Long et al., 2008).

LT-exposed cells displayed a paradoxical relation between the downregulation of photosynthesis-related gene expression and maintained cell photosynthetic capacity. Although the number of active PSI and PSII sites (Figure 3B), the rETR (Figure 3C), and the Chl content (Figure 1B) were equivalent to the Ctrl conditions, pigment synthesis- and light harvesting complex-related genes were down-regulated upon LT Cd exposure (Figure 3A). In this respect, impairment of LHCBM6 accumulation has been previously shown to lead to an overall decrease in PSII antenna size, but also to a diminished photoprotection capacity governed by LHCSR1 (Peers et al., 2009; Girolomoni et al., 2017). The downregulation of LHCBM6 in LT-exposed cells is in line with the reduction by 20% of the functional LHCII antenna size found here (Figure 3D). Because these changes in light harvesting machinery-related gene expression at LT (1) fully recovered upon Cd removal (Figure 3A) and (2) were already initiated at ST, they were likely triggered by Cd presence, and presumably as a response to the negative impact of Cd exposure. These changes probably aim to limit the production of ROS that takes place in the chloroplast when light absorption is larger than the calvin cycle capacity; the RUBISCO protein level and CO_2 fixation were shown to be massively decreased upon Cd exposure (Gillet et al., 2006; Penen et al., 2020). A large increase in Violaxanthin (Vx) content was also found at LT, which is linked to the upregulation of zeaxanthin epoxidase (Figure 3, A–E). Vx acts as antioxidant in the lipid phase of the thylakoid membrane or the protein/lipid interface (Havaux and Niyogi, 1999; Baroli et al., 2003; Havaux et al., 2007).

The apparent paradoxical observations made here at LT (no impact on growth and photochemistry; decrease in the expression of genes involved in pigment-protein light harvesting complexes; high content in antioxidant Vx), strongly indicates that the cells reached a new equilibrium where damages due to Cd exposure are under control.

P and metal homeostasis are interconnected in Chlamydomonas

Cd exposure yielded another paradoxical observation, with the downregulation of multiple P homeostasis-related genes upon Cd exposure without effect on P cellular concentration, which remained similar to control conditions (Figure 5B). This may result from the fact that among 10 type B and 4 type A Pi transporter genes identified in the Chlamydomonas genome (Moseley and Grossman, 2009), only four and five of those genes were downregulated upon ST and LT Cd exposure, respectively. The *PTA3* gene, encoding a Mn/Pi co-transporter (Fristedt et al., 1999; Jensen et al., 2003), was in contrast upregulated in ST and LT conditions (Figure 5A). As this gene is regulated by Mn deficiency, and not by P deprivation (Allen et al., 2007b), the PTA3 transporter may rather play a role in Mn over-accumulation occurring after ST and LT Cd exposure (Figure 1F).

Several lines of evidence exist that P and metal homeostasis are interconnected in photosynthetic cells. In Chlamydomonas, Cd tolerance was previously shown to depend on P concentration in the medium (Wang and Dei, 2006) and a large part of the Cd accumulated in vacuolar Ca polyphosphate granules (Penen et al., 2017). Fe, K, and Zn uptake were also influenced by P availability, whereas Cu, Fe, and Zn over-accumulated in presence of Cd under P limitation (Webster et al., 2011). The differential expression of P homeostasis-related genes under Cd exposure could therefore indirectly be the result of Cd-induced alterations of metal homeostasis. This connection was observed in Arabidopsis where Fe deficiency- and P starvation-regulated genes showed a significant overlap (Li and Lan, 2015), in a similar trend as observed for Chlamydomonas in this study: to an upregulation of Fe deficiency genes upon Fe starvation corresponded a downregulation of P genes (Figures 5, A and 6, A).

In Arabidopsis, the P starvation response is mainly under the control the of PHR1 and PHR1-like (PHL1) TFs (Bustos et al., 2010). Furthermore, some Fe deficiency-responsive genes repressed under P starvation in WT plants were misregulated in the *phr1phl1* double mutant, suggesting an involvement of these TFs in Fe deficiency-responsive gene expression (Briat et al., 2015; Hanikenne et al., 2021). PHR1 also plays a role in Zn and P homeostasis coordination (Khan et al., 2014), suggesting that this TF is involved in the homeostasis of various nutrients.

In Chlamydomonas, the PSR1 TF is homologous to PHR1 (Rubio et al., 2001) and its role in P starvation response is well conserved (Wykoff et al., 1999; Moseley et al., 2006). Our study shows that the regulatory function of these TFs in metal homeostasis is also conserved since nine metal homeostasis-related genes are part of the PSR1 regulatory network in Chlamydomonas (Figure 7). This is further supported by the apparently conserved regulatory link between (1) PHR1 and the chloroplastic ferritin encoding gene *FER1* in Arabidopsis (Bournier et al., 2013) and (2) PSR1 and both genes (*FER1* and *FER2*) encoding the two chloroplastic ferritin subunits in Chlamydomonas (Figure 7). Moreover, a *psr1* mutant displayed altered metal accumulation, both in control conditions and upon Cd exposure (Figure 8B), and reduced expression of putative metal homeostasis gene targets (Figure 8A), further highlighting the function of PSR1 in metal homeostasis. In particular, the *psr1* mutant internalized less Cd (Figure 8C), which is in agreement with the downregulation of *PSR1* upon ST and LT Cd exposure that could contribute to cell preservation (Figure 5A).

A bHLH TF is involved in Fe homeostasis and the response to Cd in Chlamydomonas

With the noticeable exception of CRR1 and its key role in Cu homeostasis (Kropat et al., 2005), metal homeostasis regulation by TFs remains poorly described in Chlamydomonas, especially for Fe, although the involvement of a bHLH TF (Cre05.g241636) was proposed based on its upregulation

Downloaded from https://academic.oup.com/plphys/advance-article/doi/10.1093/plphys/kiab375/6353050 by guest on 24 August 2021

upon Fe deficiency and its homology to Arabidopsis group IVc of bHLH (Urzica et al., 2012; Zhang et al., 2015; Li et al., 2016a; Liang et al., 2017; Naranjo-Arcos et al., 2017). This hypothesis is supported by (1) the observation that seven out of the nine Fe homeostasis genes included in our promoter analysis are putative targets of this bHLH TF (Figure 7), including all genes of the high affinity Fe^{3+} uptake system (see above) and (2) by the mis-regulation of Fe-related genes in a *bhlh* mutant in Ctrl condition (Figure 8A). Interestingly, *FSD1* (encoding an FeSOD), whose transcript level and corresponding enzymatic activity are decreased under Fe deficiency (Allen et al., 2007b), as well as the genes encoding the Cu transporter CTR2, the Zn transporter ZRT1, and the Mn transporter NRAMP1, are all putatively targeted by this bHLH TF, suggesting that it may play a more general role in metal homeostasis. The reduced accumulation of Cu, Zn, and Mn in a *bhlh* mutant exposed to Cd supports this hypothesis (Figure 8B). The mutant also accumulated less Cd and displayed higher photosynthesis efficiency (Figure 8, C and E), together with maintained growth, in the presence of Cd. As for *IRT1*, this is a paradox: the induction of the Cre05.g241636 gene by Cd might per se be detrimental for the cells by possibly sustaining Cd uptake. However, this negative side effect may be the cost of enabling maintained Fe, and possibly other metal, homeostasis, which is critical for the cells, in the presence of Cd.

If the Cre05.g241636 bHLH TF is important to control metal homeostasis and is induced upon Cd exposure, it is not essential for the induction of Fe deficiency genes (Figure 8A) or to maintain Fe cellular levels in the presence of Cd (Figure 8B) and putative targets are induced in the *bhlh* mutant (*FRE1*, *FSD1*, Figure 8A) in control conditions possibly compensating the mutation, all suggesting that additional regulators are likely to be involved in Fe homeostasis regulation in Chlamydomonas. In Arabidopsis, Fe homeostasis regulation is orchestrated by multiple bHLH TFs such as FIT, POPEYE (PYE), and subgroup Ib bHLHs (bHLH38/39/100/101; Colangelo and Guerinot, 2004; Long et al., 2010; Wang et al., 2013). Acting upstream of bHLH Ib and FIT TFs, the bHLH IVc TFs are functionally redundant and play a primary role in Fe homeostasis regulation (Zhang et al., 2015; Li et al., 2016a; Liang et al., 2017; Naranjo-Arcos et al., 2017), whereas the MYB10 and MYB72 TFs act downstream of the bHLH TFs and are important for Fe allocation in Arabidopsis (Palmer et al., 2013). MYB72 was shown to be induced by Cd exposure (Lešková et al., 2017). However, in Chlamydomonas, Cre05.g241636 is the only bHLH TF related to the Arabidopsis group IVc of bHLHs and no other bHLH was found to be responsive to Fe or other metal deficiency (Urzica et al., 2012; Urzica, 2017). Thus, the induction of Fe-deficiency genes in the *bhlh* mutant in response to Cd must be controlled by other TFs. Interestingly, two MYB TFs were found to be putative targets of Cre05.g241636 (Figure 7). The Cre10.g421021 MYB gene was upregulated upon ST exposure and downregulated in Recovery, whereas the Cre14.g633789 MYB gene had an expression dynamic similar to the Cre05.g241636 bHLH (upregulated in ST and LT but downregulated in Recovery). In addition, the GCN5-related N-acetyltransferases NAT30 (Cre13.g581150) previously shown to be induced by Fe deficiency (Urzica et al., 2012) was upregulated in the ST/LT conditions but downregulated in Recovery, as Cre07.g331475, another GCN5-related *N*-acetyltransferases coding gene (Supplemental Dataset S1). Since these proteins are involved in gene expression regulation through histone acetylation, and as homologs were shown to control Fe homeostasis in Arabidopsis (Xing et al., 2015), such epigenetic modifications may also play a role in metal homeostasis regulation in Chlamydomonas.

The PSR1 and Cre05.g241636 bHLH TFs are interconnected in a conserved regulatory network

PSR1, the main regulator of P homeostasis in Chlamydomonas (Wykoff et al., 1999; Moseley et al., 2006), may also be involved in the regulation of Fe and metal homeostasis genes. We showed here that it forms a putative regulatory network with the Cre05.g241636 bHLH TF (Figure 7). This is in agreement with the recent report showing that the two proteins interact in a regulatory complex controlling P homeostasis and triacylglycerol metabolism genes (Hidayati et al., 2019). Through mutant analysis, we confirmed here that both TFs control the expression of several metal homeostasis genes, including *IRT1* and *FEA2* (Figure 8A). Our in silico analysis of mis-regulated genes in *fit* and *phr1phl1* Arabidopsis mutants supports that such a regulatory network was at least partly conserved, then diversified, during the evolution of land plants (Supplemental Dataset S4 and Supplemental Figure S5). Not only are deficiency responses for Cu, Fe, or P relying on conserved TFs and signaling processes (Wykoff et al., 1999; Rubio et al., 2001; Kropat et al., 2005; Bustos et al., 2010; Bernal et al., 2012; Urzica et al., 2012), but our work also indicates that a coordinated regulation of these responses is conserved over a large evolutionary time in the plant lineage.

Overall, this network effectively links the homeostasis of different metals (Fe, Cu, Zn, Mn) and P in Chlamydomonas. It is mobilized and is required during LT acclimation to Cd. Further work will be required to dissect in detail these interactions, in the absence and presence of Cd. Our work dramatically expands our molecular understanding of (1) the response to chronic exposure to Cd, a highly toxic and persistent pollutant posing a major environmental threat and (2) the integrated regulatory control of nutrient homeostasis in photosynthetic cells.

Materials and methods

Strain and growth conditions

Chlamydomonas (*C. reinhardtii*) strain CC-4403 (Chlamydomonas Resource Center, Duke University) was cultivated in 25-mL culture in modified TAP medium (Harris et al., 2009) where inorganic phosphate was replaced by β-glycerophosphate (TAgP) to avoid Cd-P complex formation (Collard and Matagne, 1990), buffered to pH 7.0 with glacial

Downloaded from https://academic.oup.com/plphys/advance-article/doi/10.1093/plphys/kiab375/6353050 by guest on 24 August 2021

acetic acid and sterilized by autoclaving. The required amount of $CdCl_2$ was then added to the Erlenmeyer flasks from a stock solution (1 mM, filtered through a 0.22 μm Millipore filter). Cultures were grown under continuous photosynthetic photon flux density (100 μE m^{-2} s^{-1}), at 25°C and placed on an agitator platform (110 rpm).

All Chlamydomonas knockout mutants (Supplemental Table S3) were provided by the CLiP (https://www.chlamylibrary.org/; Li et al., 2016b) and were genotyped by PCR (Supplemental Table S4) to confirm the presence of the insertion cassette (CIB1). The culture conditions were the same as above and the background strain CC-5325 (*cw15* mt^-) was used as control. The *psr1* and *bhlh* mutants were back-crossed with the 137c WT strain (CC-125, mt^+). The crosses, maturation of zygotes, and random analysis of meiotic products were carried out as described (Hanikenne et al., 2001).

Experimental design

Starting from pre-culture obtained from a single colony, three control cultures were set up in TAP liquid medium (control) and three cultures were set up with addition of Cd (50 μM $CdCl_2$). This Cd concentration was selected as the best compromise between an effective toxicity (25% growth reduction) and ensuring the survival of the cells over a long period of time. Each culture was transferred into fresh medium with a starting OD_{750} of ∼0.005 (corresponding to ∼5 × 10^4 cells/mL) every 7 d for 6 months.

After this period, two transition conditions were tested in addition to the control and LT Cd exposure (Supplemental Figure S1): (1) the three control cultures were duplicated and one duplicate of each culture was exposed to 50 μM Cd for 3 d and (2) the three Cd-treated cultures were duplicated and one duplicate of each culture was grown for 3 d in TAgP medium free of Cd. After three days of growth, the four triplicated conditions (control, exposed for 3 d, exposed for 6 months, and grown without Cd for 3 d after a 6-month exposure) were sampled for further analysis.

Cell density and Chl quantification

The cell density was estimated by OD_{750} in a spectrophotometer (ThermoScientific, Genesys 20). The Chls were quantified using optical density measurements as follows. A sample of 200 μL of culture was centrifuged 1 min at 2,500*g* and the pigments were extracted by adding 800 μL of 100% ethanol. The mix was centrifuged at maximum speed (>12,000*g*) for 1 min and 400 μL of supernatant were used to measure the OD_{650} on a 96-well plate on a fluorimeter (Fluorometer Perkin Elmer 1420, Multilabel Counter Victor 3). The Chl $a+b$ (μg/mL) content was then calculated by multiplying the OD_{650} by 25.11 (correction factor) and normalized according to the culture cell density.

Tolerance test on agar plates

Two-day-old liquid cultures (∼5 × 10^6 cells/ml) were diluted to 10^6, 10^5, and 10^4 cells/mL in fresh TAgP medium. Drops of 10 μL or 15 μL of each cell concentration were spotted on TAgP 1.5% (w/v) agar (agar M, Sigma-Aldrich) plates containing 0 μM, 200 μM, 300 μM, 400 μM, 500 μM, and 600 μM Cd, respectively. The plates were then exposed to 100 μE m^{-2} s^{-1} at 25°C for 10 d. Pictures of the plates were regularly captured.

Metal quantification by inductively coupled plasma atomic emission spectroscopy

Ten milliliter of 3-d-old cell culture (OD_{750} ∼0.7, corresponding to ∼7 × 10^6 cells/ml) grown in TAgP liquid medium in the presence or absence of 50 μM Cd were sampled and centrifuged at 2,000 × g for 5 min. The supernatant was then discarded and the pellet sequentially washed with 5 ml of 1 mM EDTA (twice) and 5 ml of distilled water. After each washing step, the cells were resuspended by manual shaking and centrifuged for 5 min at 2,500 *g* and the supernatant discarded. A cell digestion was then realized by the addition of 3 ml of 65% HNO_3 to the pellet, which was then resuspended by manual shaking and stored for 2 d at 4°C; 7 ml of distilled water and 200 μl of 65% HNO_3 were then added to the tubes and the mixture was used for mineral element profiling by inductively coupled plasma atomic emission spectroscopy as described (Nouet et al., 2015).

Pigment quantification by high pressure liquid chromatography

Pigments were extracted on ice from 1 mL of 7-d-old cell culture (OD_{750} ∼1.9, corresponding to ∼2 × 10^7 cells/mL). Samples were centrifuged for 2 min at 2,000*g* and the pellet was resuspended in 90% methanol and frozen at −80°C.

The microtubes containing the pigments were centrifuged for 2 min at 13,000*g* and the supernatant was filtered using a 0.2 μm PTFE filter (Acrodisc CR, PALL). Then, 200 μL of filtered supernatant were transferred to high pressure liquid chromatography (HPLC) vial. The analysis was realized on a column C-18 (Nova-Pack, silica-based, particle of 4 μm, length of 150 mm and inner diameter of 3.9 mm, Waters, WATO36975). The equipment (Shimadzu) consisted of an injector (SIL-20AC), a pump (LC-20AT), a degassing unit (DGC-20A5R), an oven (CTO-10ASVP) in which the column was located, a holder with a photodiode array (SPD-M20A) and a communication module (CBM-20A). The Empower software (Waters, version 6.1.2154.917) was used to control the HPLC, collect, and analyze the data. The analyses were carried out at 25°C with a flow of 1 mL/min. The mobile phase composition varied during the analysis as three solutions were used following a gradient mode: (1) solution A (90% methanol + ammonium acetate 100 mM); (2) solution B (90% acetonitrile); and (3) solution C (100% ethyl acetate). The quantification was based on peak area at 430 nm after having averaged measures of standard solutions (DHI Labo Products).

Downloaded from https://academic.oup.com/plphys/advance-article/doi/10.1093/plphys/kiab375/6353050 by guest on 24 August 2021

Photosynthesis measurements

In vivo, Chl fluorescence and time-resolved absorption change measurements were performed at room temperature (25°C) using a JTS-10 spectrophotometer (Bio-logic, France) or a SpeedZen Fluorescence imaging system (BeamBio, Uani, France) and actinic light was provided by light sources peaking at 640 nm or 520 nm, respectively. For all experiments, cells grown in low photosynthetic photon flux density (PPFD) (50 µE photons m^{-2} s^{-1}) were harvested during exponential growth phase (OD_{750} approximately 0.3–0.5, (corresponding to approximately 3–5 × 10^6 cells/mL) and concentrated to a concentration of 10 µg Chls/mL in fresh TAP medium.

The apparent photochemical yield of PSII (ΦPSII) was calculated as $(F_m' - F_s)/F_m'$, where F_s is the fluorescence level excited by actinic light (I_{lum}), and F_m' is the maximum fluorescence emission level induced by a 150 ms superimposed saturating pulse (>3,500 µE m^{-2} s^{-1}). The relative electron transfer rate was obtained as $rETR_{II} = \Phi PSII \times I_{lum}$ (Genty et al., 1989).

The ratio between active PSI and PSII centers was estimated from the amplitude of the fast phase (<1 ms) of the electrochromic shift (ECS) signal (at 520–546 nm) after illumination with a single-turnover laser flash. The contribution of PSII was calculated from the decrease in the ECS amplitude after the flash upon the addition of the PSII inhibitors 3-(3,4-dichlorophenyl)-1,1-dimethylurea (DCMU, 20 µM) and hydroxylamine (1 mM), whereas the contribution of PSI corresponded to the amplitude of the ECS that was insensitive to these inhibitors (Roberty et al., 2014).

PSI relative content was also assessed by measuring maximal P_{700} absorption change in the presence of DCMU (20 µM) with a probing light peaking at 705 nm (6 nm full width at half maximum). In order to remove nonspecific contributions to the signal at 705 nm, absorption changes measured at 740 nm (10 nm full width at half maximum) were subtracted (Godaux et al., 2015).

Functional PSII antenna size was measured as the rate of Chl fluorescence induction from open (F_0) to closed PSII centers (F_m) in the presence of DCMU (20 µM), to block reoxidation of the PSII electron acceptor QA (Joliot and Joliot, 2006).

RNA extraction, library preparation, and illumina sequencing

A volume equivalent to 5 × 10^7 cells was sampled and centrifuged 5 min at 2,000*g*. The pellet was then resuspended in 2 mL of TAgP, transferred in an eppendorf microtube and centrifuged for 5 min at 2,500*g*. The supernatant was discarded and the pellet immediately frozen in liquid nitrogen and stored at −80°C.

First, cells were mechanically disrupted using glass beads for one minute at 25 Hz in a grinder (Retsch, MM 200). Total RNA was then extracted using the NucleoSpin RNA Plant (Macherey-Nagel). The quantity and quality were assessed using a Nanodrop (Nanovue plus spectrophotometer).

Libraries for RNA-Seq were prepared from 1 µg of total RNAs with the TruSeq Stranded mRNA Library Prep Kit (Illumina, San Diego, CA, USA), multiplexed and sequenced with an Illumina NextSeq500 device (high throughput mode; 75-bp single-end reads, ∼20 million reads/sample).

Transcriptomic analysis

Read quality was assessed using FASTQC (v.0.10.1, http://www.bioinformatics.babraham.ac.uk/projects/fastqc/). Quality trimming and removal of adapters were performed using TRIMMOMATIC (v.0.32; Bolger et al., 2014), with the following parameters: trim bases with quality score lower than Q26 in 5′ and 3′ of reads; remove any reads with Q < 26 in any sliding window of 10 bases; crop 1 base in 3′ of all reads, and discard reads shorter than 70 bases, and resulted in the loss of ∼8% of the reads. The resulting high quality reads were then aligned on *Chlamydomonas* strain CC-503 reference genome V5, downloaded from Phytozome (https://phytozome.jgi.doe.gov) on September 16, 2016, using TopHat (v2.1.1; Trapnell et al., 2009), with the following parameters: –read-mismatches 2; –min-intron-length 40; –max-intron-length 2,000; –report-secondary-alignments; –no-novel-juncs and providing an indexed genome annotation file. The aligned reads were counted using htseq-count (v0.6.1p1; Anders et al., 2015).

DEGs were identified by pairwise comparisons with the DESeq2 package (v.1.12.3; Love et al., 2014). Genes were retained as differentially expressed when the $\log_2$ fold-change was > 1 or < −1, with a FDR (Benjamini–Hochberg) adjusted P <0.05.

GO enrichments were carried out using GOseq as implemented in the run_GOseq.pl perl script of the Trinity suite (Grabherr et al., 2011).

The consistency of the RNA-Seq data analysis was confirmed by RT-qPCR applied to a selection of genes (Supplemental Figure S9).

Promoter scanning for TFBSs

The promoter sequence (1,000-bp upstream from transcription start site) of each DEG of the Recovery response was extracted from *Chlamydomonas* reference genome V5 using bedtools (Quinlan and Hall, 2010). This dataset was searched for the presence of motifs corresponding to the TFBS of the PSR1 and Cre05.g241636 TFs *A. thaliana* homologs retrieved from PlantTFDB (Jin et al., 2017). The analysis was carried out using the FIMO tool (Grant et al., 2011) from the MEME suite (Bailey et al., 2009). A regulatory link was inferred based on the presence of a TFBS in the promoter sequence of a gene (P < 0.05) and the resulting network was visualized in Cytoscape (Shannon et al., 2003). The promoter sequences (1,500-bp upstream to 100-bp downstream from transcription start site) of the Arabidopsis genes analysed in Supplemental Dataset S4 were extracted from the TAIR10 (Lamesch et al., 2012) assembly using Araport11 (Cheng et al., 2017) annotation and bedtools (Quinlan and Hall, 2010). The motif enrichment analysis in these promoters was

Downloaded from https://academic.oup.com/plphys/advance-article/doi/10.1093/plphys/kiab375/6353050 by guest on 24 August 2021

carried out using the AME tool (McLeay and Bailey, 2010) from the MEME suite and the TFBS from PlantTFDB as above.

RT-qPCR analysis

One microgram of total RNA extracted as described above was used for cDNA synthesis with Oligo dT and RevertAid H Minus Kit (Thermo Fisher Scientific, Belgium). RT-qPCR experiments were carried out on a QuantStudio 5 machine (Applied Biosystems, Foster City, CA, USA) using Takyon qPCR Kits for Probe Assay (Eurogentec, Belgium). Three technical replicates were run for each sample/primer combination (Supplemental Table S5) as housekeeping genes and relative gene expression levels relative to two housekeeping genes (*SSA9* and *CBPL*, Supplemental Table S5, Idoine et al., 2014; Lekeux et al., 2018) were calculated by the $2^{-\Delta\Delta Ct}$ method as described (Nouet et al., 2015).

Statistical analysis

The normality of distribution and homogeneity of variance of the data were assessed using the Shapiro–Wilk test and the Levene test as implemented in R, respectively. If both conditions were not fulfilled, a pairwise *t* test was carried out to evaluate significant differences between treatments. Otherwise, one-way ANOVA (Analysis of variance) was used, followed by a multirange Tukey's test if significant differences were detected at a 95% level of confidence.

Accession numbers

PHC18 (Cre24.g755997), TCP10 (Cre06.g303200), IRT1 (Cre12.g530400), IRT2 (Cre12.g530350), bHLH (Cre05.g241636), PSR1 (Cre12.g495100), FRE1 (Cre04.g227400), FSD1 (Cre10.g436050), CTR1 (Cre13.g570600), FEA2 (Cre12.g546600), PHO1 (Cre08.g359300), PTB2 (Cre07.g325741), FLA15 (AT3G52370), AHA7 (AT3G60330), IRT1 (AT4G19690), MTP3 (AT3G58810), MGD2 (AT5G20410), PS2 (AT1G73010), PHT1;4 (AT2G38940), UGT74E2 (AT1G05680), VTL5 (AT3G25190), PHR1 (AT4G28610), PHL1 (AT5G29000), FIT (AT2G28160). The RNA-Seq reads have been deposited in the National Center for Biotechnology Information (NCBI) Sequence Read Archive (SRA) Database with BioProject identification number PRJNA608616.

Supplemental data

The following materials are available in the online version of this article.

Supplemental Figure S1. Scheme of the experimental design.

Supplemental Figure S2. Impact of Cd on the Chlamydomonas cultures.

Supplemental Figure S3. Microscopic observation illustrating multicellular structures forming under Cd exposure.

Supplemental Figure S4. Heatmap of all 577 significantly differentially expressed genes.

Supplemental Figure S5. Replicated Cd tolerance test on agar plates for *tcp10* and *phc18* mutants.

Supplemental Figure S6. Promoter analysis in nine Arabidopsis genes mis-regulated in roots of both *phr1phl1* and *fit* mutants compared to the WT.

Supplemental Figure S7. Bulked segregant analysis of the expression of predicted PSR1 target genes in the progeny resulting from a *psr1* × WT backcross.

Supplemental Figure S8. Cd tolerance in palmelloids.

Supplemental Figure S9. Validation of RNA-Seq data.

Supplemental Table S1. Genetic analysis of the *psr1* and *bHLH* mutants.

Supplemental Table S2. Statistics for pairwise comparisons of electron transport rate of PSII between WT and *bhlh* in control conditions and upon Cd exposure (50 μM) presented in Figure 8E.

Supplemental Table S3. List of CLiP mutants used in the study.

Supplemental Table S4. List of genotyping primers for the CLiP mutants.

Supplemental Table S5. List of RT-qPCR primers.

Supplemental Dataset S1. Lists of differentially expressed genes from all pairwise comparisons described in Figure 2.

Supplemental Dataset S2. Gene ontology enrichment analysis for pairwise comparisons and sub-groups described in Figure 2.

Supplemental Dataset S3. List of putative PSR1 and Cre05.g241636 bHLH targets in the recovery response, as described in Figures 2 and 7.

Supplemental Dataset S4. Analysis of the conservation of a P/Fe coordinated regulation in Arabidopsis.

ACKNOWLEDGMENTS

We thank A. Degueldre, S. Banneux, and M. Schloesser for technical support, the GIGA Genomics platform (University of Liège) for the sequencing and the Durandal cluster (InBioS-PhytoSystems, University of Liège) for computational resources.

Funding

This work was supported by the "Fonds de la Recherche Scientifique–FNRS" (PDR T.0206.13, MIS F.4511.16, CDR J.0009.17 and PDR T0120.18 to M.H.) and by the University of Liège (ARC GreenMagic to M.H. and P.C.). M.H. and P.C. are Senior Research Associates of the F.R.S.-FNRS.

Conflict of interest statement. The authors declare no competing financial interests.

References

Aguilera A, Amils R (2005) Tolerance to cadmium in *Chlamydomonas* sp. (Chlorophyta) strains isolated from an extreme acidic environment, the Tinto River (SW, Spain). Aquat Toxicol **75**: 316–329

Ahmadi H, Corso M, Weber M, Verbruggen N, Clemens S (2018) CAX1 suppresses Cd-induced generation of reactive oxygen species in *Arabidopsis halleri*. Plant Cell Environ **41**: 2435–2448

Aksmann A, Pokora W, Baścik-Remisiewicz A, Dettlaff-Pokora A, Wielgomas B, Dziadziuszko M, Tukaj Z (2014) Time-dependent

Downloaded from https://academic.oup.com/plphys/advance-article/doi/10.1093/plphys/kiab375/6353050 by guest on 24 August 2021

changes in antioxidative enzyme expression and photosynthetic activity of *Chlamydomonas reinhardtii* cells under acute exposure to cadmium and anthracene. Ecotoxicol Environ Saf **110**: 31–40

Allen MD, del Campo JA, Kropat J, Merchant SS (2007a) *FEA1*, *FEA2*, and *FRE1*, encoding two homologous secreted proteins and a candidate ferrireductase, are expressed coordinately with *FOX1* and *FTR1* in iron-deficient *Chlamydomonas reinhardtii*. Eukaryot Cell **6**: 1841–1852

Allen MD, Kropat J, Tottey S, Del Campo JA, Merchant SS (2007b) Manganese deficiency in *Chlamydomonas* results in loss of photosystem II and MnSOD function, sensitivity to peroxides, and secondary phosphorus and iron deficiency. Plant Physiol **143**: 263–277

Alterio V, Langella E, De Simone G, Monti SM (2015) Cadmium-containing carbonic anhydrase CDCA1 in marine diatom *Thalassiosira weissflogii*. Mar Drugs **13**: 1688–1697

Anders S, Pyl PT, Huber W (2015) HTSeq–a Python framework to work with high-throughput sequencing data. Bioinformatics **31**: 166–169

Bailey TL, Boden M, Buske FA, Frith M, Grant CE, Clementi L, Ren J, Li WW, Noble WS (2009) MEME Suite: tools for motif discovery and searching. Nucleic Acids Res **37**: W202–W208

Baliardini C, Meyer C-L, Salis P, Saumitou-Laprade P, Verbruggen N (2015) *CATION EXCHANGER1* cosegregates with cadmium tolerance in the metal hyperaccumulator *Arabidopsis halleri* and plays a role in limiting oxidative stress in *Arabidopsis* Spp. Plant Physiol **169**: 549–559

Baroli I, Do AD, Yamane T, Niyogi KK (2003) Zeaxanthin accumulation in the absence of a functional xanthophyll cycle protects *Chlamydomonas reinhardtii* from photooxidative stress. Plant Cell **15**: 992–1008

Bernal M, Casero D, Singh V, Wilson GT, Grande A, Yang H, Dodani SC, Pellegrini M, Huijser P, Connolly EL, et al. (2012) Transcriptome sequencing identifies SPL7-regulated copper acquisition genes FRO4/FRO5 and the copper dependence of iron homeostasis in Arabidopsis. Plant Cell **24**: 738–761

Bernard A (2008) Cadmium & its adverse effects on human health. Indian J Med Res **128**: 557–564

Blaby-Haas CE, Merchant SS (2014) Lysosome-related organelles as mediators of metal homeostasis. J Biol Chem **289**: 28129–28136

Blaby-Haas CE, Merchant SS (2012) The ins and outs of algal metal transport. Biochim Biophys Acta **1823**: 1531–1552

Bolger AM, Lohse M, Usadel B (2014) Trimmomatic: a flexible trimmer for Illumina sequence data. Bioinformatics **30**: 2114–2120

Bournier M, Tissot N, Mari S, Boucherez J, Lacombe E, Briat J-F, Gaymard F (2013) *Arabidopsis* ferritin 1 (*AtFer1*) gene regulation by the phosphate starvation response 1 (AtPHR1) transcription factor reveals a direct molecular link between iron and phosphate homeostasis. J Biol Chem **288**: 22670–22680

Boyd M, Rosenzweig F, Herron MD (2018) Analysis of motility in multicellular *Chlamydomonas reinhardtii* evolved under predation. PLoS ONE **13**: e0192184

Bräutigam A, Schaumlöffel D, Preud'homme H, Thondorf I, Wesenberg D (2011) Physiological characterization of cadmium-exposed *Chlamydomonas reinhardtii*. Plant Cell Environ **34**: 2071–2082

Briat J-F, Rouached H, Tissot N, Gaymard F, Dubos C (2015) Integration of P, S, Fe, and Zn nutrition signals in *Arabidopsis thaliana*: potential involvement of PHOSPHATE STARVATION RESPONSE 1 (PHR1). Front. Plant Sci **6**: 290

Brumbarova T, Bauer P, Ivanov R (2015) Molecular mechanisms governing Arabidopsis iron uptake. Trends Plant Sci **20**: 124–133

Busch A, Rimbauld B, Naumann B, Rensch S, Hippler M (2008) Ferritin is required for rapid remodeling of the photosynthetic apparatus and minimizes photo-oxidative stress in response to iron availability in *Chlamydomonas reinhardtii*. Plant J **55**: 201–211

Bustos R, Castrillo G, Linhares F, Puga MI, Rubio V, Pérez-Pérez J, Solano R, Leyva A, Paz-Ares J (2010) A central regulatory system largely controls transcriptional activation and repression responses to phosphate starvation in Arabidopsis. PLoS Genet **6**: e1001102

Cailliatte R, Lapeyre B, Briat J-F, Mari S, Curie C (2009) The NRAMP6 metal transporter contributes to cadmium toxicity. Biochem J **422**: 217–228

Cain JR, Allen RK (1980) Use of a cell wall-less mutant strain to assess the role of the cell wall in cadmium and mercury tolerance by *Chlamydomonas reinhardtii*. Bull Environ Contam Toxicol **25**: 797–801

Cao X, Wang H, Zhuang D, Zhu H, Du Y, Cheng Z, Cui W, Rogers HJ, Zhang Q, Jia C, et al. (2018) Roles of MSH2 and MSH6 in cadmium-induced G2/M checkpoint arrest in Arabidopsis roots. Chemosphere **201**: 586–594

Clemens S, Aarts MG, Thomine S, Verbruggen N (2013) Plant science: the key to preventing slow cadmium poisoning. Trends Plant Sci **18**: 92–99

de Carpentier F, Lemaire SD, Danon A (2019) When unity is strength: the strategies used by *Chlamydomonas* to survive environmental stresses. Cells **8**: 1307

Cheloni G, Slaveykova VI (2021) Morphological plasticity in *Chlamydomonas reinhardtii* and acclimation to micropollutant stress. Aquat Toxicol **231**: 105711

Chen Z-H, Nimmo GA, Jenkins GI, Nimmo HG (2007) BHLH32 modulates several biochemical and morphological processes that respond to Pi starvation in Arabidopsis. Biochem J **405**: 191–198

Cheng C-Y, Krishnakumar V, Chan AP, Thibaud-Nissen F, Schobel S, Town CD (2017) Araport11: a complete reannotation of the *Arabidopsis thaliana* reference genome. Plant J **89**: 789–804

Clemens S (2019) Safer food through plant science: reducing toxic element accumulation in crops. J Exp Bot **70**: 5537–5557

Clemens S, Antosiewicz DM, Ward JM, Schachtman DP, Schroeder JI (1998) The plant cDNA LCT1 mediates the uptake of calcium and cadmium in yeast. Proc Natl Acad Sci USA **95**: 12043–12048

Clemens S, Ma JF (2016) Toxic heavy metal and metalloid accumulation in crop plants and foods. Annu Rev Plant Biol **67**: 489–512

Colangelo EP, Guerinot ML (2004) The essential basic helix-loop-helix protein FIT1 is required for the iron deficiency response. Plant Cell **16**: 3400–3412

Collard JM, Matagne RF (1990) Isolation and genetic analysis of *Chlamydomonas reinhardtii* strains resistant to cadmium. Appl Environ Microbiol **56**: 2051–2055

Crist RH, Martin JR, Carr D, Watson JR, Clarke HJ, Carr D (1994) Interaction of metals and protons with algae. 4. Ion exchange vs adsorption models and a reassessment of scatchard plots; ion-exchange rates and equilibria compared with calcium alginate. Environ Sci Technol **28**: 1859–1866

Domozych DS, Domozych CE (2014) Multicellularity in green algae: upsizing in a walled complex. Front Plant Sci **5**: 649

Duncan L, Nishii I, Harryman A, Buckley S, Howard A, Friedman NR, Miller SM (2007) The *VARL* gene family and the evolutionary origins of the master cell-type regulatory gene, *regA*, in *Volvox carteri*. J Mol Evol **65**: 1–11

Duy D, Stübe R, Wanner G, Philippar K (2011) The chloroplast permease PIC1 regulates plant growth and development by directing homeostasis and transport of iron. Plant Physiol. **155**: 1709–1722

Duy D, Wanner G, Meda AR, von Wirén N, Soll J, Philippar K (2007) PIC1, an ancient permease in Arabidopsis chloroplasts, mediates iron transport. Plant Cell **19**: 986–1006

Faller P, Kienzler K, Krieger-Liszkay A (2005) Mechanism of $Cd2^+$ toxicity: $Cd2^+$ inhibits photoactivation of Photosystem II by competitive binding to the essential $Ca2^+$ site. Biochim Biophys Acta **1706**: 158–164

Fristedt U, van Der Rest M, Poolman B, Konings WN, Persson BL (1999) Studies of cytochrome *c* oxidase-driven H^+-coupled phosphate transport catalyzed by the *Saccharomyces cerevisiae* Pho84 permease in coreconstituted vesicles. Biochemistry **38**: 16010–16015

Downloaded from https://academic.oup.com/plphys/advance-article/doi/10.1093/plphys/kiab375/6353050 by guest on 24 August 2021

Gaur JP, Rai LC (2001) Algal Adaptation to Environmental Stresses. Springer, Berlin, Heidelberg, pp. 363–388

Genty B, Briantais J-M, Baker NR (1989) The relationship between the quantum yield of photosynthetic electron transport and quenching of chlorophyll fluorescence. Biochim Biophys Acta Biomemb **990**: 87–92

Gillet S, Decottignies P, Chardonnet S, Maréchal PL (2006) Cadmium response and redoxin targets in *Chlamydomonas reinhardtii*: a proteomic approach. Photosynth Res **89**: 201–211

Girolomoni L, Ferrante P, Berteotti S, Giuliano G, Bassi R, Ballottari M (2017) The function of LHCBM4/6/8 antenna proteins in *Chlamydomonas reinhardtii*. J Exp Bot **68**: 627–641

Glaesener AG, Merchant SS, Blaby-Haas CE (2013) Iron economy in *Chlamydomonas reinhardtii*. Front Plant Sci **4**: 337

Godaux D, Bailleul B, Berne N, Cardol P (2015) Induction of photosynthetic carbon fixation in anoxia relies on hydrogenase activity and proton-gradient regulation-like1-mediated cyclic electron flow in *Chlamydomonas reinhardtii*. Plant Physiol **168**: 648–658

Grabherr MG, Hass BJ, Yassour M, Levin JZ, Thompson DA, Amit I, Adiconis X, Fan L, Raychowdhury R, Zeng Q, et al. (2011) Full-length transcriptome assembly from RNA-Seq data without a reference genome. Nat Biotechnol **29**: 644–652

Grant CE, Bailey TL, Noble WS (2011) FIMO: scanning for occurrences of a given motif. Bioinformatics **27**: 1017–1018

Hallmann A (2003) International Review of Cytology. Academic Press, MA, USA, pp 131–182

Hallmann A (2006) The pherophorins: common, versatile building blocks in the evolution of extracellular matrix architecture in Volvocales. Plant J **45**: 292–307

Hanikenne M (2003) *Chlamydomonas reinhardtii* as a eukaryotic photosynthetic model for studies of heavy metal homeostasis and tolerance. New Phytol **159**: 331–340

Hanikenne M, Esteves SM, Fanara S, Rouached H (2021) Coordinated homeostasis of essential mineral nutrients: a focus on iron. J Exp Bot **72**: 2136–2153

Hanikenne M, Krämer U, Demoulin V, Baurain D (2005a) A comparative inventory of metal transporters in the green alga *Chlamydomonas reinhardtii* and the Red Alga *Cyanidioschizon merolae*. Plant Physiol **137**: 428–446

Hanikenne M, Matagne RF, Loppes R (2001) Pleiotropic mutants hypersensitive to heavy metals and to oxidative stress in *Chlamydomonas reinhardtii*. FEMS Microbiol Lett **196**: 107–111

Hanikenne M, Merchant SS, Hamel P (2009) Chapter 10 - transition metal nutrition: a balance between deficiency and toxicity. *In* EH Harris, DB Stern, GB Witman, eds, The Chlamydomonas Sourcebook Ed 2. Academic Press, London, pp 333–399

Hanikenne M, Motte P, Wu MCS, Wang T, Loppes R, Matagne RF (2005b) A mitochondrial half-size ABC transporter is involved in cadmium tolerance in *Chlamydomonas reinhardtii*. Plant Cell Environ **28**: 863–873

Harris EH, Stern DB, Witman GB (2009) The Chlamydomonas Sourcebook, Ed 2. Academic Press, London

Hartwig A (2010) Mechanisms in cadmium-induced carcinogenicity: recent insights. Biometals **23**: 951–960

Havaux M, Dall'Osto L, Bassi R (2007) Zeaxanthin has enhanced antioxidant capacity with respect to all other xanthophylls in Arabidopsis leaves and functions independent of binding to PSII antennae. Plant Physiol **145**: 1506–1520

Havaux M, Niyogi KK (1999) The violaxanthin cycle protects plants from photooxidative damage by more than one mechanism. Proc Natl Acad Sci USA **96**: 8762–8767

Haynes RJ (1980) Ion exchange properties of roots and ionic interactions within the root apoplasm: their role in ion accumulation by plants. Bot Rev **46**: 75–99

He XL, Fan SK, Zhu J, Guan MY, Liu XX, Zhang YS, Jin CW (2017) Iron supply prevents Cd uptake in *Arabidopsis* by inhibiting *IRT1* expression and favoring competition between Fe and Cd uptake. Plant and Soil **416**: 453–462

Heim MA, Jakoby M, Werber M, Martin C, Weisshaar B, Bailey PC (2003) The basic helix–loop–helix transcription factor family in plants: a genome-wide study of protein structure and functional diversity. Mol Biol Evol **20**: 735–747

Herbik A, Bölling C, Buckhout TJ (2002) The involvement of a multicopper oxidase in iron uptake by the green algae *Chlamydomonas reinhardtii*. Plant Physiol **130**: 2039–2048

Hessen DO, Van Donk E, Andersen T (1995) Growth responses, P-uptake and loss of flagellae in *Chlamydomonas reinhardtii* exposed to UV-B. J Plankton Res **17**: 17–27

Hidayati NA, Yamada-Oshima Y, Iwai M, YamanoT, KajikawaM, SakuraiN SudaK SesokoK HoriK ObayashiT, et al. (2019) Lipid remodeling regulator 1 (LRL1) is differently involved in the phosphorus-depletion response from PSR1 in *Chlamydomonas reinhardtii*. Plant J **100**: 610–626

Howe G, Merchant S (1992) Heavy metal-activated synthesis of peptides in *Chlamydomonas reinhardtii*. Plant Physiol **98**: 127–136

Idoine AD, Boulouis A, Rupprecht J, Bock R (2014) The diurnal logic of the expression of the chloroplast genome in *Chlamydomonas reinhardtii*. PLoS One **9**: e108760

Iwasa K, Murakami S (1969) Palmelloid formation of *Chlamydomonas* II. Mechanism of palmelloid formation by organic acids. Physiol Plant **22**: 43–50

Jamers A, Coen WD (2009) Effect assessment of the herbicide paraquat on a green alga using differential gene expression and biochemical biomarkers. Environ Toxicol Chem **29**: 893–901

Jensen LT, Ajua-Alemanji M, Culotta VC (2003) The *Saccharomyces cerevisiae* high affinity phosphate transporter encoded by *PHO84* also functions in manganese homeostasis. J Biol Chem **278**: 42036–42040

Jeong J, Cohu C, Kerkeb L, Pilon M, Connolly EL, Guerinot ML (2008) Chloroplast Fe(III) chelate reductase activity is essential for seedling viability under iron limiting conditions. Proc Natl Acad Sci USA **105**: 10619–10624

Jin J, Tian F, Yang D-C, Meng Y-Q, Kong L, Luo J, Gao G (2017) PlantTFDB 4.0: toward a central hub for transcription factors and regulatory interactions in plants. Nucleic Acids Res **45**: D1040–D1045

Joliot P, Joliot A (2006) Cyclic electron flow in C3 plants. Biochim Biophys Acta **1757**: 362–368

Khan GA, Bouraine S, Wege S, Li Y, de Carbonnel M, Berthomieu P, Poirier Y, Rouached H (2014) Coordination between zinc and phosphate homeostasis involves the transcription factor PHR1, the phosphate exporter PHO1, and its homologue PHO1;H3 in Arabidopsis. J Exp Bot **65**: 871–884

Khona DK, Shirolikar SM, Gawde KK, Hom E, Deodhar MA, D'Souza JS (2016) Characterization of salt stress-induced palmelloids in the green alga, *Chlamydomonas reinhardtii*. Algal Res **16**: 434–448

Kirk MM, Stark K, Miller SM, Müller W, Taillon BE, Gruber H, Schmitt R, Kirk DL (1999) *regA*, a *Volvox* gene that plays a central role in germ-soma differentiation, encodes a novel regulatory protein. Development **126**: 639–647

Kropat J, Tottey S, Birkenbihl RP, Depège N, Huijser P, Merchant S (2005) A regulator of nutritional copper signaling in *Chlamydomonas* is an SBP domain protein that recognizes the GTAC core of copper response element. Proc Natl Acad Sci USA **102**: 18730–18735

Krzesłowska M (2011) The cell wall in plant cell response to trace metals: polysaccharide remodeling and its role in defense strategy. Acta Physiol Plant **33**: 35–51

La Fontaine S, Quinn JM, Nakamoto SS, Page MD, Göhre V, Moseley JL, Kropat J, Merchant S (2002) Copper-dependent iron assimilation pathway in the model photosynthetic eukaryote *Chlamydomonas reinhardtii*. Eukaryot Cell **1**: 736–757

Lamesch P, Berardini TZ, Li D, Swarbreck D, Wilks C, Sasidharan R, Muller R, Dreher K, Alexander DL, Garcia-Hernandez M, et al. (2012) The Arabidopsis information resource (TAIR): improved gene annotation and new tools. Nucleic Acids Res **40**: D1202–D1210

Downloaded from https://academic.oup.com/plphys/advance-article/doi/10.1093/plphys/kiab375/6353050 by guest on 24 August 2021

Lane TW, Morel FMM (2000) A biological function for cadmium in marine diatoms. Proc Natl Acad Sci USA **97**: 4627–4631

Lavoie M, Fortin C, Campbell PGC (2012) Influence of essential elements on cadmium uptake and toxicity in a unicellular green alga: the protective effect of trace zinc and cobalt concentrations. Environ Toxicol Chem **31**: 1445–1452

Lavoie M, Le Faucheur S, Fortin C, Campbell PGC (2009) Cadmium detoxification strategies in two phytoplankton species: metal binding by newly synthesized thiolated peptides and metal sequestration in granules. Aquat Toxicol **92**: 65–75

Lekeux G, Laurent C, Joris M, Jadoul A, Jiang D, Bosman B, Carnol M, Motte P, Xiao Z, Galleni M, et al. (2018) di-Cysteine motifs in the C-terminus of plant HMA4 proteins confer nanomolar affinity for zinc and are essential for HMA4 function in vivo. J Exp Bot **69**: 5547–5560

Lešková A, Giehl RFH, Hartmann A, Fargašová A, von Wirén N (2017) Heavy metals induce iron deficiency responses at different hierarchic and regulatory levels. Plant Physiol **174**: 1648–1668

Li C, Zheng C, Fu H, Zhai S, Hu F, Naveed S, Zhang C, Ge Y (2021) Contrasting detoxification mechanisms of Chlamydomonas reinhardtii under Cd and Pb stress. Chemosphere **274**: 129771

Li W, Lan P (2015) Genome-wide analysis of overlapping genes regulated by iron deficiency and phosphate starvation reveals new interactions in Arabidopsis roots. BMC Res Notes **8**: 555

Li X, Zhang H, Ai Q, Liang G, Yu D (2016a) Two bHLH transcription factors, bHLH34 and bHLH104, regulate iron homeostasis in *Arabidopsis thaliana*. Plant Physiol **170**: 2478–2493

Li X, Zhang R, Patena W, Gang SS, Blum SR, Ivanova N, Yue R, Robertson JM, Lefebvre PA, Fitz-Gibbon ST, et al. (2016b) An indexed, mapped mutant library enables reverse genetics studies of biological processes in *Chlamydomonas reinhardtii*. Plant Cell **28**: 367–387

Liang G, Zhang H, Li X, Ai Q, Yu D (2017) bHLH transcription factor bHLH115 regulates iron homeostasis in *Arabidopsis thaliana*. J Exp Bot **68**: 1743–1755

de Lima MAB, Franco L de O, de Souza PM, do Nascimento AE, da Silva CAA, Maia R de CC, Rolim HML, Takaki GMC (2013) Cadmium tolerance and removal from *Cunninghamella elegans* related to the polyphosphate metabolism. Int J Mol Sci **14**: 7180–7192

Lombi E, Tearall KL, Howarth JR, Zhao F-J, Hawkesford MJ, McGrath SP (2002) Influence of iron status on cadmium and zinc uptake by different ecotypes of the hyperaccumulator *Thlaspi caerulescens*. Plant Physiol **128**: 1359–1367

Long JC, Sommer F, Allen MD, Lu S-F, Merchant SS (2008) *FER1* and *FER2* encoding two ferritin complexes in *Chlamydomonas reinhardtii* chloroplasts are regulated by iron. Genetics **179**: 137–147

Long TA, Tsukagoshi H, Busch W, Lahner B, Salt DE, Benfey PN (2010) The bHLH transcription factor POPEYE regulates response to iron deficiency in Arabidopsis roots. Plant Cell **22**: 2219–2236

Love MI, Huber W, Anders S (2014) Moderated estimation of fold change and dispersion for RNA-seq data with DESeq2. Genome Biol **15**: 550

Lurling M, Beekman W (2006) Palmelloids formation in *Chlamydomonas reinhardtii*: defence against rotifer predators? Ann Limnol Int J Lim **42**: 65–72

Macfie SM, Tarmohamed Y, Welbourn PM (1994) Effects of cadmium, cobalt, copper, and nickel on growth of the green alga *Chlamydomonas reinhardtii*: the influences of the cell wall and pH. Arch Environ Contam Toxicol **27**: 454–458

Macfie SM, Welbourn PM (2000) The cell wall as a barrier to uptake of metal ions in the unicellular green alga *Chlamydomonas reinhardtii* (Chlorophyceae). Arch Environ Contam Toxicol **39**: 413–419

Mai H-J, Pateyron S, Bauer P (2016) Iron homeostasis in *Arabidopsis thaliana*: transcriptomic analyses reveal novel FIT-regulated genes, iron deficiency marker genes and functional gene networks. BMC Plant Biol **16**: 211

McLeay RC, Bailey TL (2010) Motif Enrichment Analysis: a unified framework and an evaluation on ChIP data. BMC Bioinformatics **11**: 165

Merchant SS, Allen MD, Kropat J, Moseley JL, Long JC, Tottey S, Terauchi AM (2006) Between a rock and a hard place: trace element nutrition in Chlamydomonas. Biochim Biophys Acta **1763**: 578–594

Merchant SS, Prochnik SE, Vallon O, Harris EH, Karpowicz SJ, Witman GB, Terry A, Salamov A, Fritz-Laylin LK, Maréchal-Drouard L, et al. (2007) The Chlamydomonas genome reveals the evolution of key animal and plant functions. Science **318**: 245–250

Monteiro CM, Castro PML, Malcata FX (2011) Biomanagement of Metal-Contaminated Soils, Environmental Pollution. Springer, Dordrecht, pp. 365–385

Moseley J, Grossman AR (2009) Chapter 6 - phosphate metabolism and responses to phosphorus deficiency. *In* EH Harris, DB Stern, GB Witman, eds, The Chlamydomonas Sourcebook, Ed 2. Academic Press, London, pp. 189–215

Moseley JL, Chang C-W, Grossman AR (2006) Genome-based approaches to understanding phosphorus deprivation responses and PSR1 control in *Chlamydomonas reinhardtii*. Eukaryot Cell **5**: 26–44

Mosulén S, Domínguez MJ, Vigara J, Vílchez C, Guiraum A, Vega JM (2003) Metal toxicity in *Chlamydomonas reinhardtii*. Effect on sulfate and nitrate assimilation. Biomol Eng **20**: 199–203

Nagajyoti PC, Lee KD, Sreekanth TVM (2010) Heavy metals, occurrence and toxicity for plants: a review. Environ Chem Lett **8**: 199–216

Nagel K, Adelmeier U, Voigt J (1996) Subcellular distribution of cadmium in the unicellular green alga *Chlamydomonas reinhardtii*. J Plant Physiol **149**: 86–90

Nakamura K, Bray DF, Wagenaar EB (1975) Ultrastructure of *Chlamydomonas eugametos* palmelloids induced by chloroplatinic acid treatment. J Bacteriol **121**: 338–343

Naranjo-Arcos MA, Maurer F, Meiser J, Pateyron S, Fink-Straube C, Bauer P (2017) Dissection of iron signaling and iron accumulation by overexpression of subgroup Ib bHLH039 protein. Sci Rep **7**: 10911

Narayanan NN, Ihemere U, Chiu WT, Siritunga D, Rajamani S, Singh S, Oda S, Sayre RT (2011) The iron assimilatory protein, FEA1, from *Chlamydomonas reinhardtii* facilitates iron-specific metal uptake in yeast and plants. Front Plant Sci **2**: 67

Nishikawa K, Yamakoshi Y, Uemura I, Tominaga N (2003) Ultrastructural changes in *Chlamydomonas acidophila* (Chlorophyta) induced by heavy metals and polyphosphate metabolism. FEMS Microbiol Ecol **44**: 253–259

Nouet C, Charlier J-B, Carnol M, Bosman B, Farnir F, Motte P, Hanikenne M (2015) Functional analysis of the three HMA4 copies of the metal hyperaccumulator *Arabidopsis halleri*. J Exp Bot **66**: 5783–5795

Nouet C, Motte P, Hanikenne M (2011) Chloroplastic and mitochondrial metal homeostasis. Trends Plant Sci **16**: 395–404

Olson BJ, Nedelcu AM (2016) Co-option during the evolution of multicellular and developmental complexity in the volvocine green algae. Curr Opin Genet Dev **39**: 107–115

Page MD, Allen MD, Kropat J, Urzica EI, Karpowicz SJ, Hsieh SI, Loo JA, Merchant SS (2012) Fe sparing and Fe recycling contribute to increased superoxide dismutase capacity in iron-starved *Chlamydomonas reinhardtii*. Plant Cell **24**: 2649–2665

Page MD, Kropat J, Hamel PP, Merchant SS (2009) Two Chlamydomonas CTR copper transporters with a novel cys-met motif are localized to the plasma membrane and function in copper assimilation. Plant Cell **21**: 928–943

Palmer CM, Guerinot ML (2009) Facing the challenges of Cu, Fe and Zn homeostasis in plants. Nat Chem Biol **5**: 333–340

Palmer CM, Hindt MN, Schmidt H, Clemens S, Guerinot ML (2013) *MYB10* and *MYB72* are required for growth under iron-limiting conditions. PLoS Genet **9**: e1003953

Downloaded from https://academic.oup.com/plphys/advance-article/doi/10.1093/plphys/kiab375/6353050 by guest on 24 August 2021

Pan J, Plant JA, Voulvoulis N, Oates CJ, Ihlenfeld C (2010) Cadmium levels in Europe: implications for human health. Environ Geochem Health **32**: 1–12

Parmar P, Kumari N, Sharma V (2013) Structural and functional alterations in photosynthetic apparatus of plants under cadmium stress. Bot Stud **54**

Peers G, Truong TB, Ostendorf E, Busch A, Elrad D, Grossman AR, Hippler M, Niyogi KK (2009) An ancient light-harvesting protein is critical for the regulation of algal photosynthesis. Nature **462**: 518–521

Penen F, Isaure MP, Dobritzsch D, Bertalan I, Castillo-Michel H, Proux O, Gontier E, Le Coustumer P, Schaumlöffel D (2017) Pools of cadmium in *Chlamydomonas reinhardtii* revealed by chemical imaging and XAS spectroscopy. Metallomics **9**: 910–923

Penen F, Isaure M-P, Dobritzsch D, Castillo-Michel H, Gontier E, Le Coustumer P, Malherbe J, Schaumlöffel D (2020) Pyrenoidal sequestration of cadmium impairs carbon dioxide fixation in a microalga. Plant Cell Environ **43**: 479–495

Perreault F, Dionne J, Didur O, Juneau P, Popovic R (2011) Effect of cadmium on photosystem II activity in *Chlamydomonas reinhardtii*: alteration of O–J–I–P fluorescence transients indicating the change of apparent activation energies within photosystem II. Photosynth Res **107**: 151–157

Pinto E, Sigaud-kutner TCS, Leitão MAS, Okamoto OK, Morse D, Colepicolo P (2003) Heavy metal–induced oxidative stress in algae. J Phycol **39**: 1008–1018

Prasad MNV, Drej K, Skawińska A, Strałka K (1998) Toxicity of cadmium and copper in *Chlamydomonas reinhardtii* wild-type (WT 2137) and cell wall deficient mutant strain (CW 15). Bull Environ Contam Toxicol **60**: 306–311

Quinlan AR, Hall IM (2010) BEDTools: a flexible suite of utilities for comparing genomic features. Bioinformatics **26**: 841–842

Rachlin JW, Jensen TE, Warkentine B (1984) The toxicological response of the alga *Anabaena flos- aquae* (cyanophyceae) to cadmium. Arch Environ Contam Toxicol **13**: 143–151

Rawat I, Ranjith Kumar R, Mutanda T, Bux F (2011) Dual role of microalgae: Phycoremediation of domestic wastewater and biomass production for sustainable biofuels production. Appl Energy **88**: 3411–3424

Roberty S, Bailleul B, Berne N, Franck F, Cardol P (2014) PSI Mehler reaction is the main alternative photosynthetic electron pathway in *Symbiodinium* sp., symbiotic dinoflagellates of cnidarians. New Phytol **204**: 81–91

Rogers EE, Eide DJ, Guerinot ML (2000) Altered selectivity in an Arabidopsis metal transporter. Proc Natl Acad Sci USA **97**: 12356–12360

Rubio V, Linhares F, Solano R, Martín AC, Iglesias J, Leyva A, Paz-Ares J (2001) A conserved MYB transcription factor involved in phosphate starvation signaling both in vascular plants and in unicellular algae. Genes Dev **15**: 2122–2133

Salt DE, Baxter I, Lahner B (2008) Ionomics and the study of the plant ionome. Annu Rev Plant Biol **59**: 709–733

Samadani M, Dewez D (2018) Cadmium accumulation and toxicity affect the extracytoplasmic polyphosphate level in *Chlamydomonas reinhardtii*. Ecotoxicol Environ Saf **166**: 200–206

Satarug S, Baker JR, Urbenjapol S, Haswell-Elkins M, Reilly PEB, Williams DJ, Moore MR (2003) A global perspective on cadmium pollution and toxicity in non-occupationally exposed population. Toxicol Lett **137**: 65–83

Satarug S, Garrett SH, Sens MA, Sens DA (2010) Cadmium, environmental exposure, and health outcomes. Environ Health Perspect **118**: 182–190

Seufferheld MJ, Alvarez HM, Farias ME (2008) Role of polyphosphates in microbial adaptation to extreme environments. Appl Environ Microbiol **74**: 5867–5874

Shahid M, Dumat C, Khalid S, Niazi NK, Antunes PMC (2017) Cadmium bioavailability, uptake, toxicity and detoxification in soil-plant system. Rev Environ Contam Toxicol **241**: 73–137

Shannon P, Markiel A, Ozier O, Baliga NS, Wang JT, Ramage D, Amin N, Schwikowski B, Ideker T (2003) Cytoscape: a software environment for integrated models of biomolecular interaction networks. Genome Res **13**: 2498–2504

Sharma N, Bhalla PL, Singh MB (2013) Transcriptome-wide profiling and expression analysis of transcription factor families in a liverwort, *Marchantia polymorpha*. BMC Genomics **14**: 915

Shi L-X, Theg SM (2013) The chloroplast protein import system: From algae to trees. Biochim Biophys Acta **1833**: 314–331

Singh A, Kaur N, Kosman DJ (2007) The metalloreductase Fre6p in Fe-efflux from the yeast vacuole. J Biol Chem **282**: 28619–28626

Solti Á, Sárvári É, Tóth B, Mészáros I, Fodor F (2016) Incorporation of iron into chloroplasts triggers the restoration of cadmium induced inhibition of photosynthesis. J. Plant Physiol **202**: 97–106

Stohs SJ, Bagchi D (1995) Oxidative mechanisms in the toxicity of metal ions. Free Radic Biol Med **18**: 321–336

Stoiber TL, Shafer MM, Armstrong DE (2013) Induction of reactive oxygen species in *Chlamydomonas reinhardtii* in response to contrasting trace metal exposures. Environ Toxicol **28**: 516–523

Thomine S, Vert G (2013) Iron transport in plants: better be safe than sorry. Curr Opin Plant Biol **16**: 322–327

Toledo-Ortiz G, Huq E, Quail PH (2003) The Arabidopsis basic/helix-loop-helix transcription factor family. Plant Cell **15**: 1749–1770

Trapnell C, Pachter L, Salzberg SL (2009) TopHat: discovering splice junctions with RNA-Seq. Bioinformatics **25**: 1105–1111

Tulin F, Cross FR (2015) Cyclin-dependent kinase regulation of diurnal transcription in *Chlamydomonas*. Plant Cell **27**: 2727–2742

Urzica EI (2017) Chlamydomonas: Molecular Genetics and Physiology, Microbiology Monographs. Springer, Cham, pp. 201–231

Urzica EI, Casero D, Yamasaki H, Hsieh SI, Adler LN, Karpowicz SJ, Blaby-Haas CE, Clarke SG, Loo JA, Pellegrini M, et al. (2012) Systems and trans-system level analysis identifies conserved iron deficiency responses in the plant lineage. Plant Cell **24**: 3921–3948

Vega JM, Garbayo I, Domínguez MJ, Vigara J (2006) Effect of abiotic stress on photosynthesis and respiration in *Chlamydomonas reinhardtii*: Induction of oxidative stress. Enzyme Microb Technol **40**: 163–167

Vert G, Briat JF, Curie C (2001) *Arabidopsis IRT2* gene encodes a root-periphery iron transporter. Plant J **26**: 181–189

Vert G, Grotz N, Dédaldéchamp F, Gaymard F, Guerinot ML, Briat J-F, Curie C (2002) IRT1, an *Arabidopsis* transporter essential for iron uptake from the soil and for plant growth. Plant Cell **14**: 1223–1233

Visviki I, Rachlin JW (1994) Acute and chronic exposure of *Dunaliella salina* and *Chlamydomonas bullosa* to copper and cadmium: Effects on ultrastructure. Arch Environ Contam Toxicol **26**: 154–162

Wang N, Cui Y, Liu Y, Fan H, Du J, Huang Z, Yuan Y, Wu H, Ling H-Q (2013) Requirement and functional redundancy of Ib subgroup bHLH proteins for iron deficiency responses and uptake in *Arabidopsis thaliana*. Mol Plant **6**: 503–513

Wang T, Wu M (2006) An ATP-binding cassette transporter related to yeast vacuolar ScYCF1 is important for Cd sequestration in *Chlamydomonas reinhardtii*. Plant Cell Environ **29**: 1901–1912

Wang W-X, Dei RCH (2006) Metal stoichiometry in predicting Cd and Cu toxicity to a freshwater green alga *Chlamydomonas reinhardtii*. Environ Pollut **142**: 303–312

Warren HV (1989) Geology, trace elements and health. Soc Sci Med **29**: 923–926

Watanabe M, Henmi K, Ogawa K, Suzuki T (2003) Cadmium-dependent generation of reactive oxygen species and mitochondrial DNA breaks in photosynthetic and non-photosynthetic strains of *Euglena gracilis*. Comp Biochem Physiol C Toxicol Pharmacol **134**: 227–234

Downloaded from https://academic.oup.com/plphys/advance-article/doi/10.1093/plphys/kiab375/6353050 by guest on 24 August 2021

Webster RE, Dean AP, Pittman JK (2011) Cadmium exposure and phosphorus limitation increases metal content in the freshwater alga *Chlamydomonas reinhardtii*. Environ Sci Technol **45**: 7489–7496

Wong CKE, Cobbett CS (2009) HMA P-type ATPases are the major mechanism for root-to-shoot Cd translocation in *Arabidopsis thaliana*. New Phytol **181**: 71–78

Wu X, Santos RR, Fink-Gremmels J (2015) Cadmium modulates biofilm formation by *Staphylococcus epidermidis*. Int J Environ Res Public Health **12**: 2878–2894

Wykoff DD, Grossman AR, Weeks DP, Usuda H, Shimogawara K (1999) Psr1, a nuclear localized protein that regulates phosphorus metabolism in *Chlamydomonas*. Proc Natl Acad Sci USA **96**: 15336–15341

Xing J, Wang T, Liu Z, Xu J, Yao Y, Hu Z, Peng H, Xin M, Yu F, Zhou D, et al. (2015) GENERAL CONTROL NONREPRESSED PROTEIN5-Mediated Histone Acetylation of *FERRIC REDUCTASE DEFECTIVE3* Contributes to Iron Homeostasis in *Arabidopsis*. Plant Physiol **168**: 1309–1320.

Yadav SK (2010) Heavy metals toxicity in plants: An overview on the role of glutathione and phytochelatins in heavy metal stress tolerance of plants. S Afr J Bot **76**: 167–179

Yu Z, Wei H, Hao R, Chu H, Zhu Y (2018) Physiological changes in *Chlamydomonas reinhardtii* after 1000 generations of selection of cadmium exposure at environmentally relevant concentrations. Environ Sci Process Impacts **20**: 923–933

Yu Z, Zhang T, Zhu Y (2020) Whole-genome re-sequencing and transcriptome reveal cadmium tolerance related genes and pathways in *Chlamydomonas reinhardtii*. Ecotoxicol Environ Saf **191**: 110231

Zhang J, Liu B, Li M, Feng D, Jin H, Wang P, Liu J, Xiong F, Wang J, Wang H-B (2015) The bHLH transcription factor bHLH104 interacts with IAA-LEUCINE RESISTANT3 and modulates iron homeostasis in *Arabidopsis*. Plant Cell **27**: 787–805

Downloaded from https://academic.oup.com/plphys/advance-article/doi/10.1093/plphys/kiab375/6353050 by guest on 24 August 2021